Dynamics of N_2 fixation and fate of diazotroph-derived nitrogen in a Low Nutrient Low Chlorophyll ecosystem: results from the VAHINE mesocosm experiment (New Caledonia)

S. Bonnet[1,2], H. Berthelot[1], K. Turk-Kubo[3], S. Fawcett[4,5], E. Rahav[6,7], S. L'Helguen[8], I. Berman-Frank[6]

[1] {IRD, Aix Marseille Université, CNRS/INSU, Université de Toulon, Mediterranean Institute of Oceanography (MIO) UM 110, 13288, Marseille-Noumea, France-New Caledonia}
[2] {Mediterranean Institute of Oceanography (MIO) – IRD/CNRS/Aix-Marseille University IRD Noumea, 101 Promenade R. Laroque, BPA5, 98848, Noumea cedex, New Caledonia}
[3] {Ocean Sciences Department, University of California, Santa Cruz, USA}
[4] {Department of Geosciences, M45 Guyot Hall, Princeton University, Princeton, New Jersey 08544, USA}
[5] {Department of Oceanography, University of Cape Town, Rondebosch, 7701, South Africa}
[6] {Mina and Everard Goodman Faculty of Life Sciences, Bar-Ilan University, Ramat Gan, Israel}
[7] {National Institute of Oceanography, Israel Oceanographic and Limnological Research, Haifa, Israel}
[8] {Université de Brest, CNRS/IRD, UMR6539, Laboratoire des Sciences de l'Environnement Marin, OSU-IUEM, 29280 Plouzané, France}

Correspondence to: S. Bonnet (sophie.bonnet@ird.fr)

Abstract

N_2 fixation rates were measured daily in large (~50 m^3) mesocosms deployed in the tropical South West Pacific coastal ocean (New Caledonia) to investigate the temporal variability in N_2 fixation rates in relation with environmental parameters and study the fate of diazotroph-derived nitrogen (DDN) in a low nutrient, low chlorophyll ecosystem. The mesocosms were fertilized with ~0.8 µM dissolved inorganic phosphorus (DIP) to stimulate diazotrophy. Bulk N_2 fixation rates were replicable between the three mesocosms, averaged 18.5±1.1 nmol N L^{-1} d^{-1} over the 23 days, and increased by a factor of two during the second half of the experiment (days 15 to 23) to reach 27.3±1.0 nmol N L^{-1} d^{-1}. These later rates measured after the DIP fertilization are higher than the upper range reported for the global ocean. During the 23-days of the experiment, N_2 fixation rates were positively correlated with seawater temperature, primary production, bacterial production, standing stocks of particulate organic carbon (POC), nitrogen (PON) and phosphorus (POP), and alkaline phosphatase activity, and negatively correlated with DIP concentrations, DIP turnover time, nitrate, and dissolved organic nitrogen and phosphorus concentrations. The fate of DDN was investigated during a bloom of the unicellular diazotroph UCYN-C that occurred during the second half of the experiment. Quantification of diazotrophs in the sediment traps indicates that ~10 % of UCYN-C from the water column was exported daily to the traps, representing as much as 22.4±5.5 % of the total POC exported at the height of the UCYN-C bloom. This export was mainly due to the aggregation of small (5.7±0.8 µm) UCYN-C cells into large (100-500 µm) aggregates. During the same time period, a DDN transfer experiment based on high-resolution nanometer scale secondary ion mass spectrometry (nanoSIMS) coupled with $^{15}N_2$ isotopic labelling revealed that 16±6 % of the DDN was released to the dissolved pool and 21±4 % was transferred to non-diazotrophic plankton, mainly picoplankton (18±4 %) followed by diatoms (3±2 %). This is consistent with the observed dramatic increase in picoplankton and diatom abundances, primary production, bacterial production, and standing stocks of POC, PON, and POP during the second half of the experiment. These results offer insights into the fate of DDN during a bloom of UCYN-C in low nutrient, low chlorophyll ecosystems.

1 Introduction

Next to light, nitrogen (N) is the major limiting factor for primary productivity in much of the low-latitude surface ocean (Falkowski, 1997; Moore et al., 2013). Nitrate (NO_3^-) is the dominant form of fixed nitrogen (N) in seawater and derives from the remineralization of sinking organic N in the dark ocean. NO_3^- is supplied to photic waters by upward mixing and transport, and constitutes the main source of fixed N for photosynthetic organisms in the temperate and high latitude ocean. In the oligotrophic tropical and subtropical oceans, vertical mixing and transport of NO_3^- is generally low and surface waters are often depleted in NO_3^-.

In these ocean deserts, specialized organisms termed N_2-fixers (or diazotrophs) are able to use N in its simplest and most abundant form on Earth and in seawater, namely dinitrogen (N_2). Diazotrophs possess the nitrogenase enzyme, which cleaves the strong triple bond of the N_2 molecule to form bioavailable ammonium (NH_4^+) which is assimilated as amino acids enabling biomass growth and division. N_2 fixation thus introduces a source of new bioavailable N to surface waters, and is considered to be the most important external source of N to the ocean, more significant than atmospheric and riverine inputs (Gruber, 2004).

The dynamics of microbial communities such as diazotrophs can change abruptly in the ocean in response to small perturbations or environmental stressors. In particular, N_2 fixation has been described as a very 'patchy' process in the ocean (Bombar et al., 2015). Many factors control the distribution and activity of diazotrophs such as temperature (Bonnet et al., 2015; Moisander et al., 2010; Raveh et al., 2015; Staal et al., 2003), nutrient availability (mainly phosphate and iron) (e.g., (Mills et al., 2004)), pCO_2 ((e.g. (Levitan et al., 2007)), ambient concentrations of fixed N (NO_3^- and NH_4^+) (e.g., (Knapp et al., 2012), as well as physical forcing (e.g., (Fong et al., 2008)). Most studies dedicated to understanding the controls on marine N_2 fixation have been undertaken along large oceanic transects; these are particularly valuable and have recently led to the compilation of a global ocean database of diazotrophy (Luo et al., 2012). Spatial variability in N_2 fixation is thus far better documented and understood than temporal variability, despite the intimate connections between time and space scales in the ocean. Time-series stations with near-monthly observations set up in the late 1980's under the international JGOFS program in the subtropical North Atlantic, Pacific, and Mediterranean Sea have provided valuable data regarding the controls on N_2 fixation and its role in biogeochemical cycles on seasonal and inter-annual timescales (Dore et al., 2008; Garcia et al., 2006; Grabowski et al., 2008; Karl et al., 2012; Knapp

et al., 2005; Orcutt et al., 2001), and have also revealed novel diazotrophic microorganisms (Zehr et al., 2008) with unexpected metabolic strategies such as UCYN-A cyanobacteria that lack the oxygen-producing photosystem II complex (Tripp et al., 2010). However, fairly little attention has been paid to sub-seasonal variability in N_2 fixation and its biogeochemical drivers and consequences.

In the framework of the VAHINE (VAriability of vertical and tropHIc transfer of diazotroph derived N in the south wEst Pacific) project, we deployed three large volume mesocosms (~50 m^3, Fig. 1) in the tropical South West Pacific coastal ocean, a region known to support diazotrophy during the austral summer (Dupouy et al., 2000; Rodier and Le Borgne, 2010, 2008). Our goal was to study the high frequency temporal dynamics of N_2 fixation over short time scales (sampling every day for 23 days), in relation to hydrological parameters, biogeochemical stocks and fluxes, and the dynamics of phytoplanktonic and bacterial communities in the same water mass.

The mesocosm approach allowed us to investigate the fate of the recently fixed N_2 and its transfer from diazotrophs to non-diazotrophic organisms in this oligotrophic marine ecosystem. Diazotrophs can typically release from 10 to 50 % of their recently fixed N_2 (or diazotroph derived N, hereafter called DDN) as dissolved organic N (DON) and NH_4^+ (Glibert and Bronk, 1994; Meador et al., 2007; Mulholland et al., 2006). This exudate is potentially available for assimilation by the surrounding planktonic communities. However, such transfer of DDN to the surrounding planktonic community and its potential impact on export production is poorly understood and rarely quantified.

Over the course of this 23-day mesocosm experiment, diatom-diazotroph associations (DDAs) were the most abundant N_2 fixers during the first half of the experiment (days 2 to 14), while a bloom of the unicellular N_2-fixing cyanobacteria from Group C (UCYN-C) occurred during the second half of the experiment (days 15 to 23) (Turk-Kubo et al., 2015). Berthelot et al. (2015b) described the evolution of the C, N, and P pools and fluxes during the experiment and investigated the contribution of N_2 fixation and DON uptake to primary production and particle export. They also explored the fate of the freshly produced particulate organic N (PON), i.e., whether it was preferentially accumulated and recycled in the water column or exported out of the system. Complementary to this approach, Knapp et al. (2015) report the results of a $\delta^{15}N$ budget performed in the mesocosms to assess the dominant source of N (i.e., NO_3^- versus N_2

fixation) fueling export production during the 23-day experiment. In the present study, we focus specifically on the fate of DDN in the ecosystem during the UCYN-C bloom by studying i) the direct export of diazotrophs into the sediment traps, and ii) the transfer of DDN to non-diazotrophic plankton using high-resolution nanometer scale secondary ion mass spectrometry (nanoSIMS) coupled with $^{15}N_2$ isotopic labelling during a 72 h-process experiment.

2 Methods

2.1 Mesocosm description and sampling strategy

Three replicate large-volume mesocosms (surface 4.15 m^2, volume ~50 m^3, Fig. 1) were deployed in the oligotrophic New Caledonian lagoon, 28 km off the coast of Noumea (latitude: 22°28,855' S; longitude: 166°26,724' E) from January 13th to February 6th 2013. They consisted of large enclosures open to the air made of two 500 µm-thick films of polyethylene (PE) and vinyl acetate (EVA, 19 %), with nylon meshing in between to allow for maximum resistance and light penetration (produced by HAIKONENE KY, Finland). The mesocosm bags were 2.3 m in diameter and 15 m in height, and were equipped with removable sediment traps that enabled the collection of sinking material once a day (Fig. 1b). To alleviate any potential phosphorus limitation of diazotrophy in the mesocosms, the bags were intentionally fertilized with ~0.8 µmol L^{-1} of dissolved inorganic phosphorus (DIP) four days after the start of the experiment. A more detailed description of the mesocosms setup, the selection of the study site, and the deployment strategy can be found in Bonnet et al. (2016).

Vertical CTD profiles were performed every morning in each of the three mesocosms (hereafter referred to as M1, M2, and M3) and in the surrounding waters (hereafter referred to as lagoon waters) using a SBE Seabird CTD. All discrete samples for the parameters described below were collected daily at 7 am at three depths (1, 6, and 12 m) in each mesocosm and in the lagoon waters using braided PVC tubing (Holzelock-Tricoflex, inner diameter = 9.5 mm) connected to a Teflon PFA pump (St-Gobain Performance Plastics) activated by pressurized air. Finally, sediment trap samples were collected daily from each mesocosm by SCUBA divers.

2.2 Experimental procedures

2.2.1 N_2 fixation measurements within the mesocosms and methods intercomparison

Seawater samples for N_2 fixation rate measurements were dispensed into HCl-washed 4.5 L polycarbonate bottles that were sealed with septa and amended with $^{15}N_2$-enriched seawater (Mohr et al., 2010; Wilson et al., 2012), hereafter called the $^{15}N_2$ dissolution method. Briefly, the $^{15}N_2$-enriched seawater was prepared from 0.2 µm-filtered seawater (Sartobrand (Sartorius) cartridges) collected from the same site in a 4.5 L polycarbonate HCl-washed bottle. Seawater was first degassed through a degassing membrane (Membrana, Minimodule®, flow rate fixed at 450 mL min^{-1}) connected to a vacuum pump (<200 mbar) for at least 1 h. The bottle was then closed with a septum cap and amended with 1 mL of $^{15}N_2$ (98.9 atom% ^{15}N, Cambridge Isotopes Laboratories, Inc) per 100 mL of seawater. The bottle was shaken vigorously to fragment the $^{15}N_2$ bubble, and incubated overnight at 20 m depth at the study site (3 bars) to promote $^{15}N_2$ dissolution. The experimental bottles were amended with 5 % vol:vol $^{15}N_2$ enriched seawater (i.e., 225 mL), sealed without headspace with silicon septum caps, and incubated for 24 h on an *in situ* mooring line located close to the mesocosms at the appropriate sampling depth. After 24 h, 12 mL of the incubated seawater were subsampled into Exetainers®. These were preserved upside down in the dark at 4 °C and analyzed less than 6 months after the experiment using a Membrane Inlet Mass Spectrometer (MIMS) (Kana et al., 1994) to quantify the ^{15}N enrichment of the N_2 pool in the incubation bottles. The MIMS analyses yielded an average atom% ^{15}N for the N_2 pool of 2.4±0.2 (n=10). After collection of the Exetainer® subsamples, 2.2 L from each experiment bottle were filtered under low vacuum pressure (<100 mm Hg) onto a pre-combusted (4 h at 450 °C) GF/F filter (25 mm diameter, 0.7 µm nominal porosity) for 'bulk' N_2 fixation rate determination. The remaining volume (2.2 L) was pre-filtered through a 10 µm pore-size polycarbonate filter, and collected on a pre-combusted GF/F filter for analysis of the pico- and nanoplanktonic (<10 µm) N_2 fixation rates. Filters were stored at -20 °C until the end of the VAHINE experiment, then dried for 24 h at 60 °C before mass spectrometric analysis (see section 'Mass spectrometry analyses' below). Every day, an extra 2.2 L bottle was filled with mesocosm surface water (from ~1 m), spiked with $^{15}N_2$, and immediately filtered to determine the natural ^{15}N enrichment of the PON, which is required for calculations of N_2 fixation rates.

In the present study, we decided to use the $^{15}N_2$ dissolution method to measure N_2 fixation rates as several authors (Großkopf et al., 2012; Mohr et al., 2010; Rahav et al., 2013; Wilson et al., 2012) have reported an underestimation of rates when using the bubble method (i.e., when the $^{15}N_2$ gas is injected directly in the incubation bottle using a syringe, see below) due to incomplete equilibration of the $^{15}N_2$ gas between the headspace and the seawater in the incubation bottles compared to theoretical calculations. However, the differences observed between the two methods appear to depend on the environmental conditions (Shiozaki et al., 2015). Here, we performed an inter-comparison of both methods on day 11 in surface waters (from ~1 m) collected from M1. Briefly, seawater samples from M1 were dispensed into twelve HCl-washed 4.5 L polycarbonate bottles as described above and closed with septum caps. Six bottles were spiked with 4 mL $^{15}N_2$ (98.9 atom% ^{15}N, Cambridge isotopes Laboratories, Inc) via a gas-tight syringe, hereafter called the bubble method. Each bottle was shaken 20 times to fragment the $^{15}N_2$ bubble and facilitate its dissolution. The six remaining bottles were treated as described above for the dissolution method. All twelve bottles were then incubated for 24 h in an on-deck incubator at irradiances corresponding to the sampling depth using screening, and cooled with circulating surface seawater.

A recent study (Dabundo et al., 2014) reports potential contamination of some commercial $^{15}N_2$ gas stocks with ^{15}N-enriched NH_4^+, NO_3^- and/or nitrite (NO_2^-), and nitrous oxide (N_2O). Dabundo et al. (2014) analysed various brands of $^{15}N_2$ gas and found that the Cambridge Isotopes stock (i.e., the one used in this study) contained low concentrations of ^{15}N contaminants, and the potential overestimation of N_2 fixation rates modeled using this contamination level would range from undetectable to 0.02 nmol N L^{-1} d^{-1}. The rates measured in this study ranged from 0.5 to 69.6 nmol N L^{-1} d^{-1} suggesting that, if present, stock contamination of the magnitude reported by (Dabundo et al., 2014) would be too low to affect the results described here. To verify this, one of our $^{15}N_2$ Cambridge Isotopes batches (18/061501) was checked for contamination following the method described in Dabundo et al. (2014); it was 1.4 x 10^{-8} mol of $^{15}NO_3^-$ per mol of $^{15}N_2$ and 1.1 x 10^{-8} mol NH_4^+ per mol of $^{15}N_2$. The application of this contamination level to our samples using the model provided by Dabundo et al. (2014) indicates that our rates may only be overestimated by ~0.05 %, confirming that our present results were unaffected by possible $^{15}N_2$ stock contamination.

2.2.2 Phenotypic characterization of UCYN in the water column and the sediment traps

To investigate the direct export of UCYN-C cells during the bloom of UCYN-C that occurred in the second half of the experiment, a detailed phenotypic characterization of UCYN-C was performed at the height of the bloom (days 17 and 19), both in the water column and in the sediment traps. In parallel, UCYN-C and other diazotroph phylotypes were quantified in the sediment traps on days 17 and 19 (analytical protocols are detailed below in section 2.3).

Seawater samples for microscopic analyses were collected every day from 1, 6, and 12 m in each mesocosm in 4.5 L polycarbonate bottles as described above. Samples were immediately filtered onto 2 µm 47 mm polycarbonate filters that were fixed with paraformaldehyde (4 % final concentration) and incubated for 15 minutes at room temperature, then stored at -80 °C until microscopic analysis. Formalin-fixed sediment trap samples were homogenized and 2 ml were filtered onto 2 µm polycarbonate filters for further microscopic analyses. To characterize the phenotype of UCYN (free living cells *versus* colonies) in the mesocosms as a function of depth, we performed a detailed microscopic analysis on days 17 and 19 in M2. Note that UCYN-A cannot be observed by standard epifluorescent microscopy. Filtered samples from each depth (1, 6, and 12 m) and from the sediment traps (~15 m) were visualized using a Zeiss Axioplan (Zeiss, Jena, Germany) epifluorescence microscope fitted with a green (510-560 nm) excitation filter, which targeted the UCYN phycoerythrin-rich cells. For each filter, 47 photographs of various sections of the filter were taken at random. Each fluorescent particle was automatically delimited as a region of interest (ROI) using an in-house imageJ script. The photographs were scanned visually to remove ROIs that did not correspond to UCYN cells or UCYN aggregated cells. The area of each ROI was converted to equivalent volume assuming a spherical shape for all the aggregates. The volume of individual cells was determined from the average volume of the ROI represented by only one cell. The resultant cell volume was then used to compute the number of cells in each aggregate.

2.2.3 DDN transfer experiment

The fate of the fixed N_2 during the UCYN-C bloom (that occurred from days 15 to 23) was investigated on days 17 to 20 in M2 at 6 m. In addition to N_2 fixation measurements, seawater was sampled as described above into twelve additional 4.5 L HCl-washed polycarbonate bottles

equipped with septum caps. Full bottles were immediately amended with the dissolved $^{15}N_2$ gas (98.9 atom% ^{15}N, Cambridge Isotopes Laboratories, Inc) as described above (dissolution method), and with 1 mL of 80 g L^{-1} $NaH^{13}CO_3$ solution (99 atom% ^{13}C, Cambridge Isotopes Laboratories, Inc) and incubated *in situ* on the mooring line at 6 m-depth close to the mesocosms. After 24 h, 36 h, and 72 h of incubation (hereafter referred to as T24 h, T36 h, and T72 h), three replicate $^{15}N_2$ labelled bottles were recovered from the mooring line and subsampled for the analysis of bulk N_2 fixation rates, DDN released to the dissolved pool, abundance of targeted diazotrophs using qPCR, picophytoplankton and bacterial counts, and nanoSIMS analyses on UCYN-C and non-diazotrophs (diatoms and the 0.2-2 µm fraction) to assess the DD^{15}N transfer from diazotrophs to non-diazotrophs. All analytical protocols are detailed below in section 2.3. Three 4.5 L bottles were kept as unamended controls (i.e., without $^{15}N_2$ addition) and were immediately subsampled for the same parameters.

2.3 Analytical protocols

2.3.1 Mass spectrometry analyses

PON content and PON ^{15}N enrichment of samples collected for N_2 fixation rates determination were measured using a Delta Plus Thermo Fisher Scientific isotope ratio mass spectrometer (Bremen, Germany) coupled with an elemental analyzer (Flash EA, ThermoFisher Scientific). N_2 fixation rates were calculated according to the equations detailed in Montoya et al. (1996). Rates were considered significant when the ^{15}N enrichment of the PON was higher than three times the standard deviation obtained from T0 samples. The standard deviation was 0.004 µmol L^{-1} for PON and 0.0001 atom% for the ^{15}N enrichment.

2.3.2 Quantification of diazotrophs using qPCR in sediment traps and during the DDN transfer experiment

During the bloom of UCYN-C (days 17 and 19), immediately after sediment trap samples were collected and prior to their fixation with formalin, trap material was homogenized and fresh aliquots of 1 mL were subsampled from each jar (trap from M1, M2, and M3) and filtered onto 0.2 µm Supor (Pall-Gelman) filters, flash frozen in liquid N_2, and stored at -80 ^{o}C until analysis. For the DDN transfer experiment, after each incubation period, 2 L from each triplicate ^{13}C and $^{15}N_2$-labeled 4.5 L bottle were subsampled and filtered through 0.2 µm Supor (Pall-Gelman)

filters using gentle peristaltic pumping, and stored as described above. The abundance of eight diazotrophic phylotypes was determined using Taqman® qPCR assays: unicellular cyanobacterial groups A1 (UCYN-A1; (Church et al., 2005)), A2 (UCYN-A2; (Thompson et al., 2014)), B (UCYN-B or *Crocosphaera* spp.; (Moisander et al., 2010)), and C (UCYN-C; (Foster et al., 2007)), the filamentous, colonial cyanobacteria *Trichodesmium* spp. (Church et al., 2005), the two DDAs *Richelia* associated with both *Rhizosolenia* (het-1; (Church et al., 2005)) and *Hemiaulus* (het-2; (Foster et al., 2007)) diatoms, *Calothrix* associated with *Chaetoceros* (het-3; (Foster et al., 2007)), as well as a heterotrophic phylotype of gamma proteobacteria (γ-24474A11; (Moisander et al., 2008)). All procedures are described extensively in the companion paper by (Turk-Kubo et al., 2015). Briefly, DNA was extracted using a Qiagen DNeasy kit with modifications to recover high quality genomic DNA from cyanobacteria including a freeze thaw step, agitation and a proteinase K digestion. Extracts were tested for the presences of PCR inhibitors, compounds sometimes present in DNA extracts from the environment or introduced in the extraction process that reduce PCR efficiency, using either the UCYN-B or the UCYN-C assay. If recovery of the spiked standard template in the sample extract was <98%, the sample was considered inhibited, and diluted 1:10 with 5 kD filtered milliQ water. All extracts from the sediment traps showed inhibition when undiluted, and no inhibition when diluted 1:10. DNA extracts from the DDN transfer experiment showed no inhibition. All qPCR reactions were carried out on diluted extracts as described in (Goebel et al., 2010). The limit of detection (LOD) and limit of quantitation (LOQ) was 250 and 2000 *nif*H copies mL^{-1}, respectively, for the sediment trap samples. The LOD and LOQ for DDN transfer experiment samples was 29 and 229 *nif*H copies L^{-1}, respectively.

2.3.3 Quantification of the net release of DDN to the dissolved pool during the DDN transfer experiment

After each incubation period, 60 mL from each $^{15}N_2$-labeled 4.5 L bottle were subsampled and filtered through pre-combusted (4 h, 450 °C) GF/F filters and immediately frozen for later quantification of ^{15}N release (i.e., DDN release) to the total dissolved N pool (TDN; i.e., the sum of NO_2^-, NO_3^-, NH_4^+, and DON). The dissolved N was oxidized to NO_3^- using the persulfate oxidation method of Knapp et al. (2005) with the amendments of Fawcett et al. (2011). Briefly, 1 mL of potassium persulfate oxidizing reagent (POR) was added to duplicate 5 mL aliquots of

each subsample in 12 mL pre-combusted glass Wheaton vials, and to triplicate vials containing varying quantities of two L-glutamic acid standards, USGS-40 and USGS-41 (Qi et al., 2003) used to ensure complete oxidation and quantify the POR-associated N blank. The POR was made by dissolving 6 g of sodium hydroxide and 6 g of four-times recrystallized, methanol-rinsed potassium persulfate in 100 mL of ultra-high purity water (DIW). Sample vials were capped tightly after POR addition, and autoclaved at 121°C for 55 minutes on a slow-vent setting. The entire oxidation protocol was performed in duplicate (yielding a total of 4 oxidized aliquots for each subsample).

The concentration of the resultant NO_3^- (i.e., TDN + the POR-associated N blank) was measured by chemiluminescence (Braman and Hendrix, 1989), after which the TDN isotopic composition was determined using the 'denitrifier method', wherein denitrifying bacteria that lack N_2O reductase quantitatively convert sample NO_3^- to N_2O (Casciotti et al., 2002; Sigman et al., 2001). The denitrifying bacteria (see below) are extremely sensitive to pH; care was thus taken to lower sample pH to 7-8 after POR oxidation via the addition of 12N ACS grade HCl. The ^{15}N enrichment of the N_2O was measured by GC-IRMS using a Delta V isotope ratio mass spectrometer and custom-built on-line N_2O extraction and purification system. The international reference materials, IAEA-N3, USGS-34, USGS-32, and an in-house N_2O standard were run in parallel to monitor bacterial conversion and mass spectrometry, and each oxidized sample was analyzed twice. The final TDN concentration and ^{15}N atom% were corrected for the N blank associated with the POR. The DDN released to the TDN pool was calculated according to: ^{15}N release (nmol L^{-1} d^{-1}) = ($^{15}N_{ex}$ x TDN_{con})/N_{sr}, where $^{15}N_{ex}$ is the atom% excess of the TDN for a given time point; the TDN_{con} is the TDN concentration measured at each time point, and N_{sr} is the ^{15}N enrichment of the source pool (N_2) in the experimental bottles (i.e., 2.4±0.2 atom% ^{15}N; see above).

2.3.4 Picophytoplankton and bacteria counts during the DDN transfer experiment

After each incubation period, 3.6 mL from each $^{15}N_2$-lableled 4.5 L bottle were subsampled into cryotubes, fixed with paraformaldehyde (2 % final concentration), flash frozen in liquid N_2, and stored at -80°C until analysis. Picoplanktonanalyses were carried out at the PRECYM flow cytometry platform (https://precym.mio.univ-amu.fr/). Samples were analyzed using a FACSCalibur (BD Biosciences, San Jose, CA). For heterotrophic bacterial abundance (BA), 1.8

mL of seawater was fixed with formaldehyde (2 % final concentration, 15 minutes incubation at room temperature in the dark), frozen and stored in liquid N_2 until analysis in the laboratory. After thawing, 0.3 mL of each samples was incubated with SYBR Green II (Molecular Probes, final conc. 0.05 % [v / v], for 15 minutes at room temperature in the dark), for the nucleic acid staining, according to Marie et al. (2000). Cells were characterized by 2 main optical signals: side scatter (SSC), related to cell size, and green fluorescence (530/40), related to nucleic acids staining. Based on these criteria, two subsets of bacteria (referred to low- and high nucleic acid-containing, or LNA and HNA, respectively) were optically resolved in all samples based on their green fluorescence intensity (Gasol et al., 1999). Just before analysis, 2 µm beads (Fluoresbrite YG, Polyscience), used as an internal control, and TruCount beads (BD Biosciences), used to determine the volume analyzed, were added to the samples. To assess autotrophic picoplankton abundances, the red fluorescence (670LP, related to chlorophyll *a* content) was used as trigger signal and phytoplankton cells were characterized by 3 other optical signals: forward scatter (FSC, related to cell size), side scatter (SSC, related to cell structure), and the orange fluorescence (580/30, related to phycoerythrin content). The 2 µm beads (Fluoresbrite YG, Polyscience) were also used to discriminate picoplankton (< 2 µm) from nanoplankton (> 2 µm) populations. The flow rate was estimated by weighing 3 tubes of samples before and after a 3 minutes run of the cytometer. The cells concentration was determined from both Trucount beads and flow rate measurements. All data were collected in log scale and stored in list mode using the CellQuest software (BD Biosciences). Data analysis was performed *a posteriori* using SUMMIT v4.3 software (Dako). on a FACScalibur flow cytometer (BD Biosciences, Franklin Lakes, NJ) at the Regional Flow Cytometry Platform for Microbiology (PRECYM) (https://precym.mio.univ-amu.fr/). Standard protocols (Marie et al., 1999) were used to enumerate phytoplankton and heterotrophic prokaryotes. Samples were thawed at room temperature in the dark, homogenized by gentle shaking, and filtered through 20 µm strainers in order to avoid large aggregates clogging the instrument fluidics. Just before analysis, 1 mL of sample was transferred into a flow cytometry tube, and 10 µL of a 2 µm fluorosphere (Fluoresbryte^{TM}, Polysciences) solution were added. These beads were used both as an internal control, and to discriminate cell clusters. Flow cytometric analyses of heterotrophic prokaryotes required pre-staining with a fluorescent nucleic acid probe, SYBR® Green I (Sigma, Germany), at a 1:1000 v/v final dilution of the commercial solution (excitation 488 nm/emission 530 nm). Prior to analysis, samples were incubated with

SYBR® Green I for 15 minutes in the dark at room temperature. Side scatter (SSC) was used as trigger signal and SYBR® Green I green fluorescence was collected in the green range of 510-550 nm. Combining SYBR® Green I fluorescence and light scattering unambiguously distinguishes cells from inorganic particles, detritus, and free DNA (Marie et al., 1999).

2.3.5 Microscopic cell counts during the DDN transfer experiment

Microscopic cell counts. In parallel with the picoplankton counts, diatoms, dinoflagellates, and ciliates were enumerated from 100 mL subsamples collected from each mesocosm that were preserved in Lugol's solution following the Utermöhl method (Hasle, 1978). Cells were counted on a Nikon Eclipse TE2000-E inverted microscope equipped with phase-contrast and a long distance condenser. All groups were quantified in each sample, and diatoms were identified to the lowest possible taxonomic level to examine potential community composition changes and help us to prioritize nanoSIMS analyses.

2.3.6 NanoSIMS analyses and ^{13}C and ^{15}N assimilation rates during the DDN transfer experiment

nanoSIMS analyses. After each incubation period (24, 36 and 72 h), 250 mL from each labeled 4.5 L bottle were subsampled, fixed with 25 mL of paraformaldehyde (2 % final concentration) and incubated for 24 h at 4 °C, then filtered successively through 25 mm diameter 10 µm, 2 µm, and 0.2 µm pore size polycarbonate filters and rinsed with 0.2 µm filtered seawater. All filters were then sputtered with gold and palladium to ensure conductivity prior to nanoSIMS analyses. Diatoms and UCYN-C were analysed on the 10 µm filters, and the picoplanktonic (0.2-2 µm) fraction was analysed on the 0.2 µm filters. Diatoms were easily recognized on the CCD (charge coupled device) camera of the nanoSIMS, as were UCYN-C that formed large aggregates of cells, facilitating their recognition for nanoSIMS targeted analyses. However, we cannot exclude the possibility that some UCYN-B were analysed, despite being present at very low abundances, i.e., almost two orders of magnitude less abundant than UCYN-C (Fig. 5) in the analysed samples. Several analyses were performed for each group of cells of interest (an average of ~25 cells analysed for UCYN-C and diatoms, and between 62 and 140 cells analysed for the 0.2-2 µm fraction per time point) to assess the variability of their isotopic composition. A total of ~400 individual cells were analysed by nanoSIMS in this experiment to ensure the robustness of the

data. NanoSIMS analyses were performed on a N50 (Cameca, Gennevilliers France) at the French National Ion MicroProbe Facility according to methods previously described (Bonnet et al., Accepted). A 1.3-3 pA 16 keV Cesium (Cs^+) primary beam focused onto a ~100 nm spot diameter was scanned on a 256 x 256 or 512 x 512 pixel raster (depending on the raster areas, which ranged from 15 µm x 15 µm to 50 µm x 50 µm) with a counting time of 1 ms per pixel. Samples were implanted with Cs^+ prior to analysis to remove surface contaminants and increase conductivity. For diatoms, the pre-implant was longer and with higher voltage (2-5 min, 17 pA) to penetrate the silica shell. Negative secondary ions $^{12}C^-$, $^{13}C^-$, $^{12}C^{14}N^-$, $^{12}C^{15}N^-$, and $^{28}Si^-$ were detected with electron multiplier detectors, and secondary electrons were imaged simultaneously. Ten to fifty serial quantitative secondary ion mass planes were generated and accumulated in the final image. Mass resolving power was ~8000 in order to resolve isobaric interferences. Data were processed using the look@nanosims software package (Polerecky et al., 2012). All scans were first corrected for any drift of the beam during acquisition, and C and N isotope ratio images were created by adding the secondary ion counts for each recorded secondary ion for each pixel over all recorded planes and dividing the total counts by the total counts of a selected reference mass. Individual cells were easily identified in nanoSIMS secondary electron, $^{12}C^-$, $^{12}C^{14}N^-$, and ^{28}Si images that were used to define regions of interest (ROI) around individual cells (^{28}Si data are not presented here). For each ROI, the ^{15}N and ^{13}C enrichments were calculated.

^{15}N assimilation rates were calculated for individual cells analysed by nanoSIMS. Our goal was to determine the biological compartment to which the ^{15}N had been transferred. These were performed after 24 h of incubation. Calculations were performed as follows (Foster et al., 2011; Foster et al., 2013): Assimilation (mol N $cell^{-1}$ d^{-1}) = ($^{15}N_{ex}$ x N_{con})/N_{sr}, where $^{15}N_{ex}$ is the excess atom% of the individual cells measured by nanoSIMS after 24 h of incubation; the N_{con} is the N content of each cell determined as described below, and N_{sr} is the ^{15}N enrichment of the source pool (N_2) in the experimental bottles (i.e. 2.4±0.2 atom% ^{15}N in this experiment). The cell-specific N assimilation rate was then multiplied by the cell number enumerated for each group of phytoplankton and bacteria by microscopy and flow cytometry. Standard deviations were calculated using the variability of ^{15}N enrichment measured by nanoSIMS on replicate cells and the standard deviation of the estimated cellular N content (see below) of UCYN-C, non-diazotrophic phytoplankton, and bacteria. Final standard deviations were calculated according to propagation of errors laws.

To determine the N_{con} of diatoms, cell cross section, apical and transapical dimensions were measured on the dominant diatom species present in the mesocosms and analysed by nanoSIMS to calculate biovolumes. All dimensions were measured on at least 20 cells using a Nikon Eclipse TE2000-E inverted microscope equipped with phase-contrast and a long distance condenser. Dimensions were entered into the international diatom data base (Leblanc et al., 2012) in which bio-volumes are calculated following the geometric model of each cell type as described in (Sun and Liu, 2003). Carbon (C) content (C_{con}) was then calculated for the species of interest using the equations of (Eppley et al., 1970) and (Smayda, 1978). For *Synechococcus* spp. and picoeukaryotes, we used C_{con} data from Fu et al. (2007) (249±21 fg C $cell^{-1}$) and Yentsch and Phinney (1985) (2100 fg $cell^{-1}$), respectively. C_{con} was then converted to N_{con} using the Redfield ratio of 6.6:1 (Redfield, 1934). For bacteria, an average N_{con} of 5.8±1.5 fg N $cell^{-1}$ (Fukuda et al., 1998) was used. For UCYN-C, cell dimensions were measured and the bio-volume was calculated based on the equations reported in Sun and Liu (2003). C_{con} was then calculated using the relationship between bio-volume and C_{con} (Verity et al., 1992) (22 pg $cell^{-1}$). C_{con} was then converted to N_{con} (2.3 pg $cell^{-1}$) using a ratio of 8.5:1 (Berthelot et al., 2015a).

2.4 Statistical analyses

Spearman correlation coefficients were used to examine the relationships between N_2 fixation rates, hydrological, biogeochemical, and biological variables in the mesocosms (n=57 to 61, α=0.05). The methods used to analyze the parameters reported in the correlation table are described in detail in companion papers in this issue (Berthelot et al., 2015b; Bonnet et al., 2016; Leblanc et al., 2016; Turk-Kubo et al., 2015).

A non-parametric Mann-Whitney test (α=0.05) was used to compare the means of N_2 fixation rates obtained using the dissolution and the bubble method, as well as to compare the means of N_2 fixation between the different phases of the experiment, mean isotopic ratios between $^{15}N_2$-enriched and natural abundance of N (0.366 atom%), and mean isotopic ratios between T24 h and T72 h in the DDN transfer experiment.

3 Results

3.1 N_2 fixation rates in the mesocosms

Bulk N_2 fixation rates averaged 18.5±1.1 nmol N L^{-1} d^{-1} throughout the 23 days of the experiment in the three mesocosms (all depths averaged together) (Table 1). The variance between the three mesocosms was low, and the temporal dynamics of the rates were similar (Fig. 2, Table 1), indicating good replicability between the mesocosms. Based on our data on N_2 fixation dynamics, we could identify three main periods during the experiments. These three periods were also defined by Berthelot et al. (2015b) based on biogeochemical characteristics and by Turk-Kubo et al. (2015) based on changes in abundances of targeted diazotrophs. During the first period (P0; from day 2 to 4, i.e., prior to the DIP fertilization), the average bulk N_2 fixation rate for the three mesocosms was 17.9±2.5 nmol N L^{-1} d^{-1} (Fig. 2a). These N_2 fixation rates decreased significantly ($p<0.05$) by ~40 % from day 5 to ~15 (hereafter called P1) to 10.1±1.3 nmol N L^{-1} d^{-1}, then increased significantly ($p<0.05$) from day 15 until the end of the experiment (day 15 to 23, hereafter called P2) to an average of 27.3±1.0 nmol N L^{-1} d^{-1} (Fig. 2a). Maximum rates were reached during P2 (between days 18 and 21) with 69.7, 67.7 and 60.4 nmol N L^{-1} d^{-1} in M1 (12 m), M2 (6 m) and M3 (12 m), respectively. From day ~15 to 21, N_2 fixation rates were higher at 12 m depth than in the surface. The difference was significant in M2 and M3 ($p<0.05$), but not in M1 ($p>0.05$). Size fractionation experiments indicate that 37±7 % of the measured N_2 fixation was associated with the <10 µm size fraction (Fig. 2b), and N_2 fixation rates in this fraction followed the same temporal trend as bulk N_2 fixation. These data indicate that for the experiment as a whole, the majority (~63 %) of the N_2 fixation was associated with the >10 µm fraction. N_2 fixation rates measured in the lagoon waters were half those measured in the mesocosms, and were on average 9.2±4.7 nmol N L^{-1} d^{-1} over the 23 days of the experiment.

The Spearman correlation matrix (Table 2) indicates that N_2 fixation was positively correlated with seawater temperature in the mesocosms, which was not the case in lagoon waters, although temperature was exactly the same inside and outside the mesocosms (from 25.4°C to 26.8°C) (Bonnet et al., 2016). N_2 fixation in the mesocosms was also positively correlated with particulate organic carbon (POC), PON, and particulate organic phosphorus (POP) (except in M2) concentrations, Chl *a* concentrations, primary production, bacterial production, alkaline phosphatase activity (APA), and *Synechococcus*, picoeukaryote and nanoeukaryote (except in

M2) abundances. N_2 fixation was negatively correlated with NO_3^-, DIP, DON, dissolved organic phosphorus (DOP) (except in M2) concentrations and DIP turn-over time.

The intercomparison between the bubble and dissolution methods performed on day 11 in M2 indicates that rates determined for the 6 replicates were 7.2±0.8 nmol N L^{-1} d^{-1} and 6.4±2.0 nmol N L^{-1} d^{-1} for the dissolution method and the bubble method, respectively, demonstrating that, at least in this study, N_2 fixation rates were not significantly different ($p>0.05$) between the two methods.

3.2 Phenotypic characterization of UCYN by microscopy

The average size of the UCYN-C cells present in the mesocosms was 5.7±0.8 µm (n=17). Both free-living and aggregated UCYN-C cells were observed in the water columns of the mesocosms. However, the detailed microscopic analysis performed on day 17 and day 19 in M2 (during the bloom of UCYN-C) (Fig. 3) indicates that the proportion of free-living cells (ROI characterized by one cell or two cells defined as dividing cells) was low (<1 % on day 17 and <5 % on day 19). The average number of UCYN-C cells per aggregate increased with depth (Fig. 3a), with the size of the aggregates reaching 50-100 µm at 6 m and 100-500 µm at 12 m depth. On day 17, the number of cells per aggregate averaged 162, 74, and 1273 at 1, 6, and 12 m, respectively. On day 19, the aggregates were much smaller (~50 µm) with only 4, 11, and 19 cells per aggregate. The sediment traps contained extremely high densities of UCYN-C cells with the average number of cells per aggregate 60 to 50,000 times higher than that measured in the water column aggregates (Fig. 3b-e).

3.3 Quantification of diazotrophs in sediment traps

qPCR analysis confirmed that UCYN-C was the most abundant diazotroph in the sediment traps on days 17 and 19, with abundances reaching 2.7 x 10^8 to 4 x 10^9 *nif*H copies L^{-1} (Fig. 4a). UCYN-C accounted for 97.4 to 99.2 % of the total *nif*H pool quantified in the traps. Abundances were higher in M2 and M3 (1.8 x 10^9 in M2 and 3 x 10^9 *nif*H copies L^{-1} in M3) compared to M1 (2.5 x 10^8 *nif*H copies L^{-1}) on day 19. Het-1 and het-3 were always recovered in the sediment traps, albeit at lower abundances (1.8 to 8.6 x 10^6 *nif*H copies L^{-1} for het-1 and 4.9 x 10^6 to 2.8 x 10^7 *nif*H copies L^{-1} for het-3) (Fig. 4b). They represented between 0.1 and 1.8 % of the targeted *nif*H pool. UCYN-B was detected in all mesocosms on both days (except in M1 on day 19), and

UCYN-A2 and *Trichodesmium* were detected in M2 on day 17 but at low abundances (0.05 % of the total *nif*H pool) compared to the other phylotypes. Het-2 was never detected in the traps, and neither was γ24774A11 or UCYN-A1.

Using the volume of each mesocosm (Bonnet et al., 2016) and the total *nif*H copies for each diazotroph phylotype in the sedimenting material and in the water column the day before the collection of the sediment traps (Turk-Kubo et al., 2015) (assuming a sinking velocity of the exported material of ~10 m day^{-1}, Gimenez et al. (2016)), we estimated the export efficiency for each phylotype. For UCYN-C, 4.6 % and 6.5 % of the cells present in the water column were exported to the traps per 24 h on day 17 and 19, respectively (assuming one *nif*H copy per cell). For het-1, 0.3 and 0.4 % of cells were exported into the traps on day 17 and 19, for het-3, 15.5 % and 10.5 % were exported, and for UCYN-B, 37.1 % and 15.5 % of UCYN-B were exported on day 17 and 19, respectively.

3.4. DDN transfer experiment performed on day 17

Net $^{15}N_2$ uptake was 24.1±2.8 nmol N L^{-1} during the first 24 h of the DDN transfer experiment performed from days 17 to 20 (Fig. 5a). As expected, integrated $^{15}N_2$ uptake increased over the course of the experiment to reach 28.8±4.3 nmol N L^{-1} at T48 h and 126.8±35.5 nmol N L^{-1} at T72 h. The DDN quantified in the TDN pool ranged from 6.2±2.4 nmol N L^{-1} at T24 h to 9.6±1.6 nmol N L^{-1} at T72 h. Considering gross N_2 fixation as the sum of net N_2 fixation and DDN release (Mulholland et al., 2004), the DDN released to the TDN pool accounted for 7.1±1.2 to 20.6±8.1 % of gross N_2 fixation.

During the 72 h targeted experiment (Fig. 5b) the diazotroph assemblage reflected that of the mesocosms from which they were sampled: UCYN-C dominated the diazotrophic community, comprising on average 62 % of the total *nifH* pool. The other most abundant phylotypes were UCYN-A2 and het-2, which represented 18 and 13 % of the total *nif*H pool, respectively. UCYN-A1, UCYN-B, het-1, het-3, and *Trichodesmium* were also detected but together they comprised less than 8 % of the total targeted community. Phylotype abundances remained relatively stable throughout the 72 h of the experiment.

NanoSIMS analyses performed on individual UCYN-C at 24 h (Fig. 6) revealed significant ($p<0.05$) ^{13}C (1.477±0.542 atom%, n=35) and ^{15}N (1.515±0.370 atom%, n=35) enrichments relative to natural abundance, indicating that UCYN-C were actively photosynthesizing and

fixing N_2. The correlation between ^{13}C enrichment and ^{15}N enrichment was significant ($r=0.85$, $p<0.01$, Fig. 6b). NanoSIMS analyses performed on diatoms and picoplankton (Fig. 5c) also revealed significant ($p<0.05$) ^{15}N enrichment of non-diazotrophic plankton, demonstrating a transfer of DDN from the diazotrophs to other phytoplankton. Both diatoms and picoplanktonic cells were significantly ($p<0.05$) more enriched at the end of the experiment (T72 h) (0.489±0.137 atom%, n=12 for diatoms; 0.457±0.077 atom%, n=96 for picopankton) than after the first 24 h (0.408±0.052 atom%, n=23 for diatoms; 0.389±0.014 atom%, n=63 for picoplankton). Finally, the ^{15}N enrichment of picoplankton and diatoms was not significantly different ($p>0.05$) during the DDN experiment.

4 Discussion

4.1 The bubble vs. the dissolution method: an intercomparison experiment

The inter-comparison experiment performed on day 11 reveals slightly lower, yet insignificantly different ($p>0.05$) average N_2 fixation rates when using the bubble method compared to the dissolution method. This result is in accordance with some comparisons made by Shiozaki et al. (2015) in temperate waters of the North Pacific. However, a lower degree of dissolution of the $^{15}N_2$ bubble may occur in warm tropical waters such as those near New Caledonia compared to the cooler, temperate North Pacific waters. In calculating N_2 fixation rates using the dissolution method, we used the value of 2.4±0.2 atom% for the ^{15}N enrichment of the N_2 pool as measured by MIMS. For the bubble method, we used the theoretical value of 8.4 atom% calculated for seawater with a temperature of 25.5 °C and salinity of 35.3 (as was the case on day 11). If we assume that equilibration was incomplete in our experiment using the bubble method, i.e., 75 % instead of 100 % as shown by Mohr et al. (2010), we calculate higher, albeit still insignificantly ($p>0.05$) N_2 fixation rates for the bubble method (8.3±2.8 nmol N L^{-1} d^{-1}) compared to the dissolution method (7.2±0.8 nmol N L^{-1} d^{-1}), confirming that equivalent results are obtained with both methods in this ecosystem.

4.2 The temporal dynamics of N_2 fixation in the mesocosms

Average N_2 fixation rates measured in the lagoon waters (outside the mesocosms, 9.2±4.7 nmol N L^{-1} d^{-1}, Table 1) are of the same order of magnitude as those reported for the Noumea lagoon

during austral summer conditions (Biegala and Raimbault, 2008). They are within the upper range of rates reported in the global ocean database (Luo et al., 2012). Indeed, open ocean cruises performed offshore of New Caledonia in the Coral and Solomon Seas (e.g., (Bonnet et al., 2015; Garcia et al., 2007) also suggest that the South West Pacific Ocean is one of the areas with the highest N_2 fixation rates in the global ocean.

Averaged over the 23 days of the experiment, N_2 fixation rates in the mesocosms were ~ 2 fold higher (18.5±1.1 nmol N L^{-1} d^{-1}) than those measured in lagoon waters (9.2±4.7 nmol N L^{-1} d^{-1}). The maximum observed rates of >60 nmol N L^{-1} d^{-1} from days 18-21 are among the highest reported for marine waters (Luo et al., 2012). DIP concentration was the predominant difference between the ambient lagoon waters and those of the mesocosms. The mesocosms were fertilized with DIP on day 4, reaching ambient concentrations of ~0.8 µmol L^{-1} compared to lagoon waters in which DIP concentrations were typically <0.05 µmol L^{-1}. According to our experimental assumption, diazotrophy would be promoted by high concentrations of DIP. Yet, in all three mesocosms, N_2 fixation rates were negatively correlated with DIP concentrations and DIP turnover time and positively correlated with APA (Table 2). Below, we describe the scenario that likely occurred in the mesocosms, which likely explains these correlations.

During P0 (day 2 to 4), N_2 fixation rates were higher in the mesocosms than in the lagoon waters, possibly due to the reduction of turbulence in the water column facilitated by the closing of the mesocosms (Moisander et al., 1997) and/or to the reduction of the grazing pressure in the mesocosms as total zooplankton abundances were slightly lower (by a factor of 1.6) in the mesocosms compared to the lagoon waters (Hunt et al., 2016). The most abundant diazotrophs in the mesocosms at P0 were het-1 and *Trichodesmium*, which were probably the most competitive groups under the initial conditions, i.e., NO_3^- depletion (concentrations were 0.04±0.02 µmol L^{-1}, Table 3) and low DIP concentrations (0.03±0.01 µmol L^{-1}, Table 3). *Trichodesmium* is able to use organic P substrates (DOP pool) under conditions of DIP deficiency (Dyhrman et al., 2006; Sohm and Capone, 2006). 24 h after the DIP fertilization (day 5), N_2 fixation rates in the mesocosms decreased by ~40 %, reaching rates comparable to those measured in lagoon waters during P1 (day 5 to 14). Enhanced DIP availability likely enabled non-diazotrophic organisms with lower energetic requirements and higher growth rates to outcompete the diazotrophs in the mesocosms via utilization of recycled N derived from recent N_2 fixation. This is supported by the observation that nano-eukaryotes and non-diazotrophic cyanobacteria such as *Prochlorococcus*

sp. increased in abundance during P1 (Leblanc et al., 2016) in the three mesocosms when N_2 fixation rates declined (Fig. 2).

During P2 (day 15 to 23), N_2 fixation rates increased dramatically in all three mesocosms. This period was defined by a high abundance of UCYN-C, which were present in low numbers in the lagoon and within the mesocosms during P0 and P1 (Turk-Kubo et al., 2015). The increase in UCYN-C abundance was synchronous with a decrease in DIP concentrations in the mesocosms (Turk-Kubo et al., 2015): UCYN-C abundance first increased in M1 (day 11), then in M2 (day 13), and finally in M3 (day 15). In all cases, the increase in UCYN-C abundance coincided with low DIP turnover time, indicative of DIP deficiency (Berthelot et al., 2015b; Moutin et al., 2005). Under NO_3^- depletion and low DIP availability, UCYN-C appeared to be the most competitive diazotroph in the mesocosms, as they exhibited the highest maximum growth rates compared to those calculated for the other diazotrophic phylotypes for the same period (Turk-Kubo et al., 2015). Some *Cyanothece* strains possess the genes required for utilization of organic P substrates such as phosphonates (Bandyopadhyay, 2011). Thus, UCYN-C, which were the major contributors to N_2 fixation during P2 (see below), may have used DOP as a P source during this period, consistent with the negative correlation observed between N_2 fixation rates and DOP concentrations (except in M2, Table 2), and driving the significant decline in DOP concentrations observed in all three mesocosms during P2 (Berthelot et al., 2015b; Moutin et al., 2005).

While temperature was not correlated with N_2 fixation in the lagoon, we observed a significant positive correlation between these parameters in the mesocosms (Table 2), probably because some diazotrophic phylotypes present in the mesocosms and absent in the lagoon waters were particularly sensitive to seawater temperature. UCYN-C reached high abundances inside the mesocosms, but was virtually absent in the lagoon waters outside the mesocosms. Turk-Kubo et al. (2015) showed that UCYN-C abundance was positively correlated with seawater temperature, suggesting that the optimal temperature for UCYN-C growth is above 25.6 °C. This result is consistent with culture studies performed using three UCYN-C isolates from the Noumea lagoon that are closely related to the UCYN-C observed here, indicating maximum growth rates at around 30°C and no growth below 25 °C (Camps, Turk-Kubo, Bonnet, Pers. comm.). Temperature above 25.6 °C and up to 26.7°C were reached on day 12 and were maintained through to the end of the mesocosm experiment, possibly explaining why UCYN-C was not

observed during P0 (when temperature was 25.4°C) even though DIP turn-over time was low (below ~1 d) (Berthelot et al., 2015b; Moutin et al., 2005).

If low DIP concentrations and seawater temperatures greater than 25.6 °C are prerequisites for UCYN-C growth, an obvious question is why they did not thrive (despite being present at low abundances) in the lagoon waters during P2 when similar conditions prevailed. We consider three possible explanations that are discussed extensively in Turk-Kubo et al. (2015): first, it is possible that UCYN-C are sensitive to turbulence, which was likely reduced in the mesocosms compared to the lagoon waters that are susceptible to trade winds and tides. Second, grazing pressures on UCYN-C may have been reduced as total zooplankton abundances were slightly lower (by a factor of 1.6) in the mesocosms compared to those in the lagoon waters (Hunt et al., 2016). Third, the water masses outside the mesocosms changed with tides and winds; thus, it is possible that UCYN-C were absent from the water mass encountered outside the mesocosms when we sampled for this experiment.

In the mesocosms, the cell specific $^{15}N_2$ fixation rate measured on day 17 (M2) for UCYN-C was $6.3\pm2.0 \times 10^{-17}$ mol N cell^{-1} d^{-1}. Multiplying this rate by the abundance of UCYN-C indicates that UCYN-C accounted for 90±29 % of bulk N_2 fixation during that period. This is consistent with the positive correlation observed between N_2 fixation rates and UCYN-C abundances in M2 (Table 2). In M1 and M3, the correlation was also positive yet insignificant. This may have been due to the low number of UCYN-C data points, thus decreasing the sensitivity of the statistical test. Coupling between UCYN-C ^{13}C and ^{15}N incorporation was significant ($r=0.85$, $p<0.01$) (Fig. 6b) and contrasts with results reported by Berthelot et al. (2016) for UCYN-C, in which ^{13}C and ^{15}N enrichment (and thus inorganic C and N_2 fixation) was uncoupled in the cells. Based on their observations, these authors suggest that the heterogeneity in the ^{15}N and ^{13}C enrichments can be explained by a specialization of some cells that induces variability in cell-specific ^{15}N-enrichment e.g., diazocytes that contain the nitrogenase enzyme in the colonial filamentous *Trichodesmium* sp. Spatial partitioning of N_2 and C fixation by colonial unicellular types was also evidenced for diazocyte-like formation in colonial *Crocosphaera.watsonii*-like (UCYN-B) cells (Foster et al., 2013). Here, UCYN-C cells fixed both ^{13}C and ^{15}N proportionally, which suggests they did not utilize diazocytes to separate diazotrophy from photosynthesis in our experiments.

4.3 UCYN aggregation and export

Throughout the 23 days of the experiment, the majority of N2 fixation (63 %) occurred in the >10 µm size fraction, even during P2 when the small (5.7±0.8 µm) unicellular UCYN-C dominated the mesocosm diazotrophic community. These findings can be explained by the aggregation of UCYN-C cells into large (>10 µm) aggregates (Fig. 7) that were retained on 10 µm filters (Fig. 3). These large UCYN-C aggregates probably formed in part due to the presence of sticky TEP (Berman-Frank et al., 2016) or other extracellularly-released proteins, and were characterized by a high sinking velocity due to their large size (up to 500 µm in diameter) and a density greater than that of seawater (Azam and Malfatti, 2007). Their aggregation and subsequent sinking within the mesocosms likely explains why volumetric N_2 fixation rates were higher at 12 m than at the surface during P2, as well as why the size of the aggregates increased with depth, and why numerous large-size aggregates and extremely high abundances of UCYN-C were recovered in the sediment traps. Aggregation processes may have been favored by the low turbulence in the mesocosms and it would be necessary to confirm that such processes also occur in the open ocean.

Colonial phenotypes of UCYN (UCYN-B) have been observed in the water column of the North Tropical Pacific (ALOHA station) (Foster et al., 2013), but to our knowledge, this is the first time that UCYN have been detected in sediment traps. Contrary to published data (e.g. (White et al., 2012)), here we demonstrate a greater export efficiency of UCYN (~10 % exported to the traps within 24 h) compared to the export of DDAs (efficiency of 0.24 to 4.7 %). Diatoms sink rapidly and DDAs have been found in sediment traps at Station ALOHA (Karl et al., 2012; Karl et al., 1997; Scharek et al., 1999a; Sharek et al., 1999b), in the Gulf of California (White et al., 2012), and in the Amazon River plume (Subramaniam et al., 2008). In our study, we observed limited export of het-1 (*Richelia* in association with *Rhizosolenia*) and het-3 (*Calothrix*) during P2, while het-2 (*Richelia* associated with *Hemiaulus*) was never recovered in the sediment traps. This is likely because *Hemiaulus* has a lower sinking rate than *Rhizosolenia* due do its smaller size, or may be more easily grazed by zooplankton than *Rhizosolenia* or *Calothrix*, which are known to be toxic to crustaceans (Höckelmann et al., 2009). We observed only rare occurrences of *Trichodesmium* export in this study probably due to its extremely limited presence and low growth rates in the mesocosms. Direct comparisons of our export results with findings from open ocean studies should be made cautiously as our mesocosms were shallower (15 m) than typical

oceanic export studies (>100 m) and were also probably characterized by reduced turbulence (Moisander et al., 1997).

We estimate that the direct export of UCYN-C accounted for 22.4±5.5 % of the total POC exported in each mesocosm at the height of the UCYN-C bloom (day 17) and decreased to 4.1±0.8 % on day 19 (Fig. 4c, Fig. 7). This calculation is based on the total POC content measured in the sediment traps (Berthelot et al., 2015b), our C_{con} for UCYN-C estimated as described above, and published C_{con} for other diazotrophs. The corresponding export of het-1, het-3, *Trichodesmium*, and UCYN-B on day 17 based on published C_{con} (Leblanc et al., 2012; Luo et al., 2012), and using an average of three *Richelia* and *Calothrix* symbionts per diatom, accounted for 6.8±0.5, 0.5±0.02, 0.3±0.3, and 0.1±0.01 % of the POC export on day 17, respectively, and for 4.2±1.7, 0.04±0.03 of the POC export on day 19 (the contribution of *Trichodesmium* and UCYN-B to POC export on day 19 was negligible). Thus, our data emphasize that despite their small size relative to DDAs, UCYN-C are able to directly export organic matter to depth by forming densely-populated aggregates that can rapidly sink. This observation is further confirmed by the *e* ratio, which quantifies the efficiency of a system to export POC relative to primary production (*e* ratio = POC export/PP) and was significantly higher ($p<0.05$) during P2 (i.e., during the UCYN-C bloom; 39.7±24.9 %) than during P1 (i.e., when DDAs dominated the diazotrophic community; 23.9±20.2 %) (Berthelot et al., 2015b). It is also consistent with the significantly ($p<0.05$) higher contribution of N_2 fixation to export production during P2 (56±24 %, and up to 80 % at the end of the experiment) compared to P1 (47±6 %, and never exceeded 60 %) as estimated by Knapp et al. (2015) using a $\delta^{15}N$ budget for the mesocosms. Our calculated contribution of N_2 fixation to export production is very high compared to other tropical and subtropical regions where diazotrophs are present (10 to 25 %; e.g., (Altabet, 1988; Knapp et al., 2005)). However, it is consistent with the high rates of N_2 fixation measured in the enclosed mesocosms compared to those from the lagoon and other tropical pelagic studies (Luo et al., 2012). The direct export of UCYN-C and other diazotrophs cannot solely explain the high *e* ratio estimated for P2. We thus hypothesize that a fraction of the DDN export that occurred during P2 was transferred indirectly via primary utilization by non-diazotrophic plankton cells that were eventually exported to the sediment traps (Fig. 7).

4.4 DDN transfer to non-diazotrophic phytoplankton and ecological implications

The amount of DDN measured in the TDN pool during the 72 h DDN transfer experiment is higher than that reported for culture studies of *Cyanothece* populations (1.0±0.3 to 1.3±0.2 % of gross N_2 fixation (Benavides et al., 2013; Berthelot et al., 2015a)). The DDN measured in the TDN pool reflects the DDN release by diazotrophs during N_2 fixation and is likely underestimated here as a fraction of this DDN has been taken up by surrounding planktonic communities. In our experiment, other diazotrophs were present in addition to *Cyanothece*, and they may have also contributed to the dissolved pool. Moreover, unlike in culture studies, field experiments are also impacted by other exogenous factors such as viral lysis (Fuhrman, 1999) and sloppy feeding (O'Neil and Roman, 1992; Vincent et al., 2007), which may enhance N release.

This DDN release plays a critical role in the N transfer between diazotrophs and non-diazotrophs. The cell-specific uptake rates of DDN during the DDN transfer experiment were calculated for each cell analysed by nanoSIMS (diatoms and cells from the 0.2-2 µm fraction). By multiplying cell-specific N uptake rates by the cellular abundance of each group on a particular day, we could identify the specific pool (diazotrophs, dissolved pool, non-diazotrophs) into which the DD^{15}N was transferred after 24 h, and the extent to which this $^{15}N_2$ accumulated. The results are summarized in Fig. 7. After 24 h, 52±17 % of the newly fixed $^{15}N_2$ remained in the UCYN-C biomass, 16±6 % had accumulated in the dissolved N pool, and 21±4 % had been transferred to non-diazotrophic plankton. In addition, 11 % of the newly fixed $^{15}N_2$ accumulated in a pool that we refer to as 'others' (corresponding to diazotrophs other than UCYN-C and potential non-diazotrophs to which $^{15}N_2$ was transferred; these cells were not analysed by nanoSIMS due to their very low abundance). Uncertainties take into account both the variability of the ^{15}N enrichment determined on ~25 cells per group by nanoSIMS, and the uncertainty in the N content per cell measured or taken from the literature.

Within the fraction of DDN transferred to the non-diazotrophs after 24 h (21 %), we calculate that 18±4 % was transferred to picoplankton, and only 3±2 % was transferred to diatoms (Fig. 7). The ^{15}N enrichment of picoplankton and diatoms was not significantly different ($p>0.05$) in this study, but as picoplankton dominated the planktonic community in the mesocosms at the time of the DDN transfer experiment, they were the primary beneficiaries of the DDN. This is consistent

with the positive correlation between N_2 fixation rates, *Synechococcus*, and pico-eukaryote abundances in the mesocosms (Table 2), as well as with the observed dramatic increase in *Synechococcus* and pico-eukaryotes abundances (by a factor of >2 between P1 and P2) (Leblanc et al., 2016). Diatom abundances also increased in the mesocosms by a factor of 2 between P1 and P2 (largely driven by *Cylindrotheca closterium*), but this increase occurred earlier than the picoplankton increase, i.e., at the end of P1 (days 11-12). Maximum diatom abundances were reached on day 15-16 at the very beginning of P2, and then declined by day 18 to reach abundances similar to those observed during P1. These results suggest that diatoms were the primary beneficiaries of DDN in the mesocosms at the start of P2, when N_2 fixation rates and UCYN-C abundances increased dramatically. This is consistent with a previous DDN transfer study performed in New Caledonia (Bonnet et al., Accepted) during which diatoms (mainly *Cylindrotheca closterium*) advantageously competed and utilized DDN released during *Trichodesmium* blooms. When the present DDN transfer experiment was performed (days 17 to 20), diatom abundances had already declined, likely due to DIP limitation (DIP turnover time was low, i.e below 1d). We hypothesize that picoplankton were more competitive for DDN under low DIP conditions as small cells with high surface to volume ratios are known to outcompete larger cells for the available DIP (Moutin et al., 2002). Moreover, some prokaryotes from the 0.2-2 µm size-fraction can utilize DOP compounds (Duhamel et al., 2012). In this study, we could not discriminate the DDN transfer to pico-autotrophs from that to pico-heterotrophs, but it is likely that both communities took advantage of the DDN, as both primary production (Berthelot et al., 2015b) and bacterial production (Van Wambeke et al., 2015) were positively correlated with N_2 fixation rates (Table 2) and increased dramatically following the increase in N_2 fixation during P2. The standing stocks of POC, PON, and POP were also positively correlated with N_2 fixation rates, suggesting that DDN sustained productivity in the studied system.

5 Conclusions

While studies on the fate of DDN in the ocean are rare, the contribution of DDN to particle export based on the $\delta^{15}N$ signatures of exported material indicate that N_2 fixation can efficiently contribute to export production in the oligotrophic ocean (Dore et al., 2008). The export of DDN may either be direct, through the sinking of diazotrophs, or indirect, through the transfer of DDN to non-diazotrophic plankton in the photic zone that are subsequently exported.

Trichodesmium is rarely recovered in sediment traps (Walsby, 1992) and most of the research dedicated to the export of diazotrophs has focused on DDAs (Karl et al., 2012) due to their high sinking velocity. Here, we demonstrate for the first time that UCYN can efficiently contribute to POC export in oligotrophic systems, predominantly due to the aggregation of small (5.7±0.8 µm) UCYN-C cells into large aggregates, which increase in size (up to 500 µm) with depth. Our results suggest that these small (typically 3-7 µm) organisms should be considered in future studies to confirm if processes observed in mesocosms are applicable to open ocean systems.

Moreover, the experimental and analytical approach used in this study allowed for the quantification of the actual transfer of DDN to different groups of non-diazotrophic plankton in the oligotrophic ocean. Our nanoSIMS results coupled with $^{15}N_2$ isotopic labelling revealed that a significant fraction of DDN (21±4 %) is quickly (within 24 h) transferred to non-diazotrophic plankton, which increased in abundance simultaneously with N_2 fixation rates. A similar nanoSIMS study performed during a *Trichodesmium* bloom (Bonnet et al., Accepted) revealed that diatoms were the primary beneficiaries of DDN and developed extensively during and after *Trichodesmium* spp. blooms. Diatoms are efficient exporters of organic matter to depth (Nelson et al., 1995). These studies show that plankton grown on DDN in the oligotrophic ocean drive indirect export of organic matter out of the photic zone, thus revealing a previously unaccounted for conduit between N_2 fixation and the eventual export to depth of DDN from the photic zone.

Acknowledgements

Funding for this research was provided by the Agence Nationale de la Recherche (ANR starting grant VAHINE ANR-13-JS06-0002), the INSU-LEFE-CYBER program, GOPS and IRD. The authors thank the captain and crew of the R/V *Alis*. We acknowledge the SEOH diver service from Noumea, as well as the technical service of the IRD research center of Noumea for their helpful technical support together with C. Guieu, J.-M. Grisoni and F. Louis for the mesocosm design and the useful advice. We thank François Robert, Smail Mostefaoui and Rémi Duhamel from the French National Ion MicroProbe Facility hosted by the Museum National d'Histoire Naturelle (Paris) for providing nanoSIMS facilities and constant advice. We are grateful to Aude Barani and Gerald Gregori from the Regional Flow Cytometry Platform for Microbiology (PRECYM) of the Mediterranean Institute of Oceanography (MIO) for the flow cytometry analyses support. D. Sigman provided analytical support for the ^{15}N measurements. Funding to IBF was provided through a collaborative grant with SB from MOST Israel and the High Council for Science and Technology (HCST)-France, a German-Israeli Research Foundation (GIF), project number 1133-13.8/2011, and grant 2008048 from the United States-Israel Binational Science Foundation (BSF).

Author contribution: S. Bonnet designed the experiments and S. Bonnet and H. Berthelot carried them out with help from E. Rahav. S. Bonnet, H. Berthelot, K.A. Turk-Kubo, S. Fawcett and S. L'Helguen analyzed the samples. I. Berman-Frank took part in experimental planning, preparation, and implementation of the project. S. Bonnet prepared the manuscript with contributions from all co-authors.

Figure captions

Figure 1. (a) Mesocosms (~50 m^3) deployed in the framework of the VAHINE project. (b) Sediment traps screwed onto the base of the mesocosms and were sampled daily by SCUBA divers.

Figure 2. (a) Horizontal and vertical distributions of bulk N_2 fixation rates (nmol N L^{-1} d^{-1}), and (b) <10 µm N_2 fixation rates (nmol N L^{-1} d^{-1}) in M1, M2, M3, and lagoon waters. Note that N_2 fixation rates in the <10 µm fraction were not measured (lower right panel). The grey bars indicate the timing of the DIP addition on day 4.

Figure 3. (a) UCYN-C cells per aggregate in M2 on day 17 and 19. (b to e) Green excitation (510-560 nm) epifluorescent replicate micrographs of UCYN-C on day 17 taken at 1 m depth (x40) (b), 6 m depth (x40) (c), 12 m depth (x40) (d), and in the sediment traps (x10) (e). Scale bar 20 µm (b to d) and 100 µm (e).

Figure 4. (a) Abundance of UCYN-C (*nif*H copies L^{-1}) and (b) other *nif*H phylotypes (UCYN-A2, UCYN-B, *Trichodesmium*, het-1, het-3) (*nif*H copies L^{-1}) recovered in the sediment trap on day 17 and 19. (c) Proportion of POC export associated with diazotrophs in the sediment traps on day 17 in M2 (height of UCYN-C bloom).

Figure 5. Results from the DDN transfer experiment performed from day 17 to 20 in M2. (a) Temporal changes in $^{15}N_2$ uptake (white, nmol N L^{-1}) and quantification of DDN in the dissolved pool (grey) over the course of the experiment. Error bars represent the standard deviation of three independent replicate incubations. (b) Temporal changes in diazotroph abundance determined by qPCR (*nif*H gene copies L^{-1}) during the same experiment. Error bars represent the standard

deviation of triplicate incubations. (c) Summary of the nanoSIMS analyses. Measured ^{13}C and ^{15}N atom% values of non-diazotrophic diatoms (white) and picoplankton (grey) as a function of incubation time. The horizontal dashed line indicates the natural abundance of ^{15}N (0.366 atom%), and the error bars represent the standard deviation for the several cells analysed by nanoSIMS.

Figure 6. (a) Green excitation (510-560 nm) epifluorescent micrographs of UCYN-C, (b) ^{13}C and ^{15}N isotopic enrichment (atom%) in individual UCYN-C cells on day 17 in M2, (c, d) nanoSIMS images showing the ^{13}C (c) and ^{15}N (d) enrichment of individual UCYN-C cells after 24 h of incubation. The white outlines show regions of interest (ROIs), which were used to estimate the $^{13}C/^{12}C$ and $^{15}N/^{14}N$ ratios.

Figure 7. Cartoon summary of the simplified pathways of N transfer in the first trophic level of the food web and the potential impact on the sinking POC flux at the height of the UCYN-C bloom in the VAHINE mesocosm experiment.

References

Altabet, M. A.: Variations in Nitrogen Isotopic Composition between Sinking and Suspended Particles - Implications for Nitrogen Cycling and Particle Transformation in the Open Ocean, Deep Sea Research, 35, 535-554, 1988.

Aminot, A. and Kerouel, R.: Dosage automatique des nutriments dans les eaux marines. Ifremer (Ed.), 2007.

Azam, F. and Malfatti, F.: Microbial structuring of marine ecosystems, Nature Reviews Microbiology 5, 782-791, 2007.

Bandyopadhyay, A., Elvitigala, T., Welsh, E., Stöckel, J., Liberton, M., Min, H., Sherman, L. A. and Pakrasi, H. B.: Novel metabolic attributes of the genus cyanothece, comprising a group of unicellular nitrogen-fixing Cyanothece, MBio, 2, 2011.

Benavides, M., Agawin, N., Arístegui, J., Peene, J., and Stal, L.: Dissolved organic nitrogen and carbon release by a marine unicellular diazotrophic cyanobacterium, Aquatic microbial ecology, 69, 69-80, 2013.

Berman-Frank, I., Spungin, D., Rahav, E., F., V. W., Turk-Kubo, K., and Moutin, T.: Dynamics of transparent exopolymer particles (TEP) during the VAHINE mesocosm experiment in the New Caledonia lagoon, Biogeosciences Discussions, doi: doi:10.5194/bg-2015-612, 2016. 2016.

Berthelot, H., Bonnet, S., Camps, M., Grosso, O., and Moutin, T.: Assessment of the dinitrogen released as ammonium and dissolved organic nitrogen by unicellular and filamentous marine diazotrophic cyanobacteria grown in culture, Frontiers in Marine Science, 2, 2015a.

Berthelot, H., Bonnet, S., Grosso, O., Cornet, V., and Barani, A.: Transfer of diazotroph derived nitrogen towards non-diazotrophic planktonic communities: a comparative study between *Trichodesmium erythraeum*, *Crocosphaera watsonii* and *Cyanothece* sp., Biogeosciences Discussions, doi: doi:10.5194/bg-2015-607, 2016. 2016.

Berthelot, H., Moutin, T., L'Helguen, S., Leblanc, K., Hélias, S., Grosso, O., Leblond, N., Charrière, B., and Bonnet, S.: Dinitrogen fixation and dissolved organic nitrogen fueled primary production and particulate export during the VAHINE mesocosm experiment (New Caledonia lagoon), Biogeosciences, 12, 4099-4112, 2015b.

Biegala, I. C. and Raimbault, P.: High abundance of diazotrophic picocyanobacteria (< 3 µm) in a Southwest Pacific coral lagoon, Aquatic Microbial Ecology, 51, 45-53, 2008.

Bombar, D., Taylor, C. D., Wilson, S. T., Robidart, J. C., Rabines, A., Turk-Kubo, K. A., Kemp, J. N., Karl, D. M., and Zehr, J. P.: Measurements of nitrogen fixation in the oligotrophic North Pacific Subtropical Gyre using a free-drifting submersible incubation device, Journal of Plankton Research, 37, 727–739, 2015.

Bonnet, S., Berthelot, H., Turk-Kubo, K., Cornet-Bartaux, V., Fawcett, S. E., Berman-Frank, I., Barani, A., Dekaezemacker, J., Benavides, M., Charriere, B., and Capone, D. G.: Diazotroph derived nitrogen supports diatoms growth in the South West Pacific: a quantitative study using nanoSIMS, Limnology and Oceanography, Accepted. Accepted.

Bonnet, S., Moutin, T., Rodier, M., Grisoni, J. M., Louis, F., Folcher, E., Bourgeois, B., Boré, J. M., and Renaud, A.: Introduction to the project VAHINE: VAriability of vertical and tropHIc transfer of diazotroph derived N in the south wEst Pacific, Biogeosciences Discussions, doi: doi:10.5194/bg-2015-615, 2016. 2016.

Bonnet, S., Rodier, M., Turk, K., K., Germineaud, C., Menkes, C., Ganachaud, A., Cravatte, S., Raimbault, P., Campbell, E., Quéroué, F., Sarthou, G., Desnues, A., Maes, C., and Eldin, G.: Contrasted geographical distribution of N2 fixation rates and nifH phylotypes in the Coral and Solomon Seas (South-Western Pacific) during austral winter conditions, Global Biogeochemical Cycles, 29, 2015.

Braman, R. S. and Hendrix, S. A.: Nanogram nitrite and nitrate determination in environmental and biological materials by vanadium (III) reduction with chemiluminescence detection, Analytical Chemistry, 61, 2715–2718, 1989.

Casciotti, K. L., Sigman, D. M., Hastings, M. G., Böhlke, J. K., and Hilkert, A.: Measurement of the Oxygen Isotopic Composition of Nitrate in Seawater and Freshwater Using the Denitrifier Method, Analytical Chemistry, 74, 4905–4912, 2002.

Church, M. J., Jenkins, B. D., Karl, D. M., and Zehr, J. P.: Vertical distributions of nitrogen-fixing phylotypes at Stn ALOHA in the oligotrophic North Pacific Ocean, Aquatic Microbial Ecology, 38, 3-14, 2005.

Dabundo, R., Lehmann, M. F., Treibergs, L., Tobias, C. R., Altabet, M. A., Moisander, A. M., and Granger, J.: The Contamination of Commercial $^{15}N_2$ Gas Stocks with ^{15}N–Labeled Nitrate and Ammonium and Consequences for Nitrogen Fixation Measurements, PloS one, 9, e110335, 2014.

Dore, J. E., Letelier, R. M., Church, M. J., Lukas, R., and Karl, D. M.: Summer phytoplankton blooms in the oligotrophic North Pacific Subtropical Gyre: Historical perspective and recent observations, Progress in Oceanography, 76, 2-38, 2008.

Duhamel, S., Björkman, K. M., and Karl, D. M.: Light dependence of phosphorus uptake by microorganisms in the North and South Pacific subtropical gyres, Aquatic Microbial Ecology, doi: doi: 10.3354/ame01593, 2012. 2012.

Dupouy, C., Neveux, J., Subramaniam, A., Mulholland, M. R., Montoya, J. P., Campbell, L., Carpenter, E. J., and Capone, D. G.: Satellite captures trichodesmium blooms in the southwestern tropical Pacific, EOS, 81, 13-16, 2000.

Dyhrman, S. T., Chappell, D., Haley, S. T., Moffett, J. W., Orchard, E. D., Waterbury, J. B., and Webb, E. A.: Phosphonate utilization by the globally important marine diazotroph *Trichodesmium*, Nature, 439, 68-71, 2006.

Eppley, R. W., Reid, F. M. H., and Strickland, J. D. H.: Estimates of phytoplankton crop size, growth rate, and primary production, Bull. Scripps Inst. Oceanogr., 17, 33-42, 1970.

Falkowski, P. G.: Evolution of the nitrogen cycle and its influence on the biological sequestration of CO2 in the ocean. , Nature, 387, 272-275, 1997.

Fawcett, S. E., Lomas, M. W., Casey, J. R., Ward, B. B., and Sigman, D. M.: Assimilation of upwelled nitrate by small eukaryotes in the Sargasso Sea, Nature Geoscience, 4, 717-722, 2011.

Fong, A. A., Karl, D. M., Lukas, R., Letelier, R. M., Zehr, J. P., and Church, M. J.: Nitrogen fixation in an anticyclonic eddy in the oligotrophic North Pacific Ocean, ISME Journal, 2, 663-676, 2008.

Foster, R. A., Kuypers, M. M. M., Vagner, T., Paerl, R. W., Musat, N., and Zehr, J. P.: Nitrogen fixation and transfer in open ocean diatom-cyanobacterial symbioses, ISME Journal, 5, 1484-1493, 2011.

Foster, R. A., Subramaniam, A., Mahaffey, C., Carpenter, E. J., Capone, D. G., and Zehr, J. P.: Influence of the Amazon River plume on distributions of free-living and symbiotic cyanobacteria in the western tropical north Atlantic Ocean, Limnology and Oceanography, 52, 517-532, 2007.

Foster, R. A., Sztejrenszus, S., and Kuypers, M. M. M.: Measuring carbon and N_2 fixation in field populations of colonial and free living cyanobacteria using nanometer scale secondary ion mass spectrometry, Journal of Phycology, 49, 502-516, 2013.

Fu, F. X., Warner, M. E., Zhang, Y., Feng, Y., and Hutchins, D. A.: Effects of increased temperature and CO2 on photosynthesis, growth, and elemental ratios in marine Synechococcus and Prochlorococcus (Cyanobacteria), Journal of Phycology, 43, 485-496, 2007.

Fukuda, R., Ogawa, H., Nagata, T., and Koike, I.: Direct Determination of Carbon and Nitrogen Contents of Natural Bacterial Assemblages in Marine Environments Nitrogen Contents of Natural Bacterial Assemblages in Marine Environments, Applied and Environmental Microbiology, 64, 3352–3358, 1998.

Garcia, N., Raimbault, P., Gouze, E., and Sandroni, V.: Nitrogen fixation and primary production in western Mediterranean, Comptes Rendus Biologies, 329, 742-750, 2006.

Garcia, N., Raimbault, P., and Sandroni, V.: Seasonal nitrogen fixation and primary production in the Southwest Pacific: nanoplankton diazotrophy and transfer of nitrogen to picoplankton organisms, Marine Ecology Progress Series, 343, 25-33, 2007.

Gasol, J. M., Zweifel, U. L., Peters, F., Fuhrman, J. A., and Hagstrom, A.: Significance of size and nucleic acid content heterogeneity as measured by flow cytometry in natural planktonic bacteria, Applied and Environmental Microbiology, 65, 4475-4483, 1999.

Gimenez, A., Baklouti, M., Bonnet, S., and Moutin, T.: Biogeochemical fluxes and fate of diazotroph derived nitrogen in the food web after a phosphate enrichment: Modeling of the VAHINE mesocosms experiment, Biogeosciences Discussions, doi: doi:10.5194/bg-2015-611, 2016. 2016.

Glibert, P. M. and Bronk, D.: Release of dissolved organic nitrogen by marine diazotrophic cyanobacteria, *Trichodesmium* spp., Applied and Environmental Microbiology, 60, 3996-4000, 1994.

Goebel, N. L., Turk, K. A., Achilles, K. M., Paerl, R., Hewson, I., Morrison, A. E., Montoya, J. P., Edwards, C. A., and Zehr, J. P.: Abundance and distribution of major groups of diazotrophic cyanobacteria and their potential contribution to N_2 fixation in the tropical Atlantic Ocean, Environmental microbiology, 12, 3272-3789, 2010.

Grabowski, M. N. W., Church, M. J., and Karl, D. M.: Nitrogen fixation rates and controls at Stn ALOHA, Aquatic Microbial Ecology, 52, 175–183, 2008.

Großkopf, T., Mohr, W., Baustian, T., Schunck, H., Gill, D., Kuypers, M. M. M., Lavik, G., Schmitz, R. A., Wallace, G. W. R., and LaRoche, J.: Doubling of marine dinitrogen-fixation rates based on direct measurements, Nature, 488, 361-363, 2012.

Gruber, N.: The dynamics of the marine nitrogen cycle and its influence on atmospheric CO_2. In: The ocean carbon cycle and climate., Follows, M. and Oguz, T. (Eds.), Kluwer Academic, Dordrecht, 2004.

Hasle, G. R.: The inverted microscope. In: Phytoplankton Manual, Sournia, A. (Ed.), UNESCO Monographs on oceanographic methodology, Paris, 1978.

Höckelmann, C., Becher, P. G., von Reuss, S. H., and Jüttner, F.: Sesquiterpenes of the geosmin-producing cyanobacterium Calothrix PCC 7507 and their toxicity to invertebrates, Z Naturforsch, 64, 49-55, 2009.

Hunt, B. P. V., Bonnet, S., Berthelot, H., Conroy, B. J., Foster, R., and Pagano, M.: Contribution and pathways of diazotroph derived nitrogen to zooplankton during the VAHINE mesocosm experiment in the oligotrophic New Caledonia lagoon, Biogeosciences Discussions, doi: doi:10.5194/bg-2015-614, 2016. 2016.

Kana, T. M., Darkangelo, C., Hunt, M. D., Oldham, J. B., Bennett, G. E., and Cornwell, J. C.: A membrane inlet mass spectrometer for rapid high precision determination of N_2, O_2, and Ar in environmental water samples, Analytical Chemistry, 66, 4166–4170, 1994.

Karl, D. M., Church, M. J., Dore, J. E., Letelier, R., and Mahaffey, C.: Predictable and efficient carbon sequestration in the North Pacific Ocean supported by symbiotic nitrogen fixation, Proceedings of the National Academy of Sciences, 109, 1842–1849, 2012.

Karl, D. M., Letelier, R. M., Tupas, R., Dore, J., Christian, J., and Hebel, D. V.: The role of nitrogen fixation in biogeochemical cycling in the subtropical North Pacific Ocean, Nature, 388, 533-538, 1997.

Knapp, A. N., Dekaezemacker, J., Bonnet, S., Sohm, J. A., and Capone, D. G.: Sensitivity of *Trichodesmium erythraeum* and *Crocosphaera watsonii* abundance and N_2 fixation rates to varying NO_3^- and PO_4^{3-} concentrations in batch cultures, Aquatic Microbial Ecology, 66, 223-236, 2012.

Knapp, A. N., Fawcett, S. E., Martinez-Garcia, A., Leblond, N., Moutin, T., and Bonnet, S.: Nitrogen isotopic evidence for a shift from nitrate- to diazotroph-fueled export production in VAHINE mesocosm experiments, Biogeosciences Discussions, 12, 19901-19939, 2015.

Knapp, A. N., Sigman, D. M., and Lipschultz, F.: N isotopic composition of dissolved organic nitrogen and nitrate at the Bermuda Atlantic Time-series Study site, Global Biogeochemical Cycles, 19, 1-15, 2005.

Leblanc, K., Arístegui, J., Armand, L., Assmy, P., Beker, B., Bode, A., Breton, E., Cornet, V., Gibson, J., Gosselin, M.-P., Kopczynska, E., Marshall, H., Peloquin, J., Piontkovski, S., Poulton, A. J., Quéguiner, B., Schiebel, R., Shipe, R., Stefels, J., van Leeuwe, M. A., Varela, M., Widdicombe, C., and Yallop, M.: A global diatom database – abundance, biovolume and biomass in the world ocean, Earth System Science Data, 4, 149–165, 2012.

Leblanc, K., Cornet-Barthaux, V., Caffin, M., Rodier, M., Desnues, A., Berthelot, H., Turk-Kubo, K., and Héliou, J.: Phytoplankton community structure in the VAHINE MESOCOSM experiment, Biogeosciences Discussions, doi: doi:10.5194/bg-2015-605, 2016. 2016.

Levitan, O., Rosenberg, G., Šetlík, I., Šetlíkova, E., Gtigel, J., Klepetar, J., Prášil, O., and Berman-Frank, I.: Elevated CO2 enhances nitrogen fixation and growth in the marine cyanobacterium Trichodesmium, Global Change Biology, 13, 1-8, 2007.

Luo, Y. W., Doney, S. C., Anderson, L. A., Benavides, M., Bode, A., Bonnet, S., Boström, K. H., Böttjer, D., Capone, D. G., Carpenter, E. J., Chen, Y. L., Church, M. J., Dore, J. E., Falcón, L. I., Fernández, A., Foster, R. A., Furuya, K., Gómez, F., Gundersen, K., Hynes, A. M., Karl, D. M., Kitajima, S., Langlois, R. J., LaRoche, J., Letelier, R. M., Maranón, E., McGillicuddy Jr, D. J., Moisander, P. H., Moore, C. M., Mourino-Carballido, B., Mulholland, M. R., Needoba, J. A., Orcutt, K. M., Poulton, A. J., Raimbault, P., Rees, A. P., Riemann, L., Shiozaki, T., Subramaniam, A., Tyrrell, T., Turk-Kubo, K. A., Varela, M., Villareal, T. A., Webb, E. A., White, A. E., Wu, J., and Zehr, J. P.: Database of diazotrophs in global ocean: abundances, biomass and nitrogen fixation rates, Earth System Science Data 5, 47-106, 2012.

Marie, D., Partensky, F., Vaulot, D., and Brussaard, C.: Enumeration of phytoplankton, bacteria and viruses in marine samples. In: Current Protocols in Cytometry, Robinson, J. P. (Ed.), John Wiley & Sons, Inc., New York, 1999.

Meador, T. B., Aluwihare, L. I., and Mahaffey, C.: Isotopic heterogeneity and cycling of organic nitrogen in the oligotrophic ocean, Limnology and Oceanography, 52, 934-947, 2007.

Mills, M. M., Ridame, C., Davey, M., La Roche, J., and Geider, J. G.: Iron and phosphorus co-limit nitrogen fixation in the eastern tropical North Atlantic, Nature, 429, 292-294, 2004.

Mohr, W., Grosskopf, T., Wallace, D. R. W., and LaRoche, J.: Methodological underestimation of oceanic nitrogen fixation rates, PloS one, 9, 1-7, 2010.

Moisander, A. M., Beinart, A., Voss, M., and Zehr, J. P.: Diversity and abundance of diazotrophs in the South China Sea during intermonsoon, The ISME journal, 2, 954-967, 2008.

Moisander, P. H., Beinart, R. A., Hewson, I., White, A. E., Johnson, K. S., Carlson, C. A., Montoya, J. P., and Zehr, J. P.: Unicellular Cyanobacterial Distributions Broaden the Oceanic N_2 Fixation Domain, Science, 327, 1512-1514, 2010.

Moisander, P. H., Rantajarvi, E., Huttunen, M., and Kononen, K.: Phytoplankton community in relation to salinity fronts at the entrance to the Gulf of Finland, Baltic Sea, Ophelia, 46, 187-203, 1997.

Montoya, J. P., Voss, M., Kahler, P., and Capone, D. G.: A simple, high-precision, high-sensitivity tracer assay for N_2 fixation, Applied and Environmental Microbiology, 62, 986-993, 1996.

Moore, C. M., Mills, M. M. M., Arrigo, K. R., Berman-Frank, I., Bopp, L., Boyd, P. W., Galbraith, E. D., Geider, R. J., Guieu, C., Jaccard, S. L., Jickells, T. D., La Roche, J., Lenton, T. M., Mahowald, N. M., Maranon, E., Marinov, I., Moore, J. K., Nakatsuka, T., Oschlies, A., Saito, M. A., Thingstad, T. F., A., T., and O., U.: Processes and patterns of oceanic nutrient limitation, Nature Geoscience, 6, 701–710, 2013.

Moutin, T., Thingstad, T. F., Van Wambeke, F., Marie, D., Slawyk, G., Raimbault, P., and Claustre, H.: Does competition for nanomolar phosphate supply explain the predominance of the cyanobacterium *Synechococcus*?, Limnology and Oceanography, 47, 1562-1567, 2002.

Moutin, T., Van Den Broeck, N., Beker, B., Dupouy, C., Rimmelin, P., and LeBouteiller, A.: Phosphate availability controls Trichodesmium spp. biomass in the SW Pacific ocean, Marine Ecology-Progress Series, 297, 15-21, 2005.

Mulholland, M., Bronk, D. A., and Capone, D. G.: Dinitrogen fixation and release of ammonium and dissolved organic nitrogen by *Trichodesmium* IMS101, Aquatic Microbial Ecology, 37, 85-94, 2004.

Mulholland, M. R., Bernhardt, P. W., Heil, C. A., Bronk, D. A., and O'Neil, J. M.: Nitrogen fixation and regeneration in the Gulf of Mexico, Limnology and Oceanography, 51, 176-177, 2006.

Nelson, D. M., Treguer, P., Brezezinski, M. A., Leynaert, A., and Queguiner, B.: Production and dissolution of biogenic silica in the ocean: Revised global estimates, comparison with regional data and relationship to biogenic sedimentation, Global Biogeochemical Cycles, 9, 359-372, 1995.

O'Neil, J. and Roman, M. R.: Grazers and Associated Organisms of *Trichodesmium*. In: Marine Pelagic Cyanobacteria: *Trichodesmium* and other Diazotrophs, Carpenter, E. J., Capone, D.G., and Rueter, J.G. (Ed.), NATO ASI Series, Springer Netherlands, 1992.

Orcutt, K. M., Lipschultz, F., Gundersen, K., Arimoto, R., Michaels, A. F., Knap, A. H., and Gallon, J. R.: A seasonal study of the significance of N2 fixation by Trichodesmium spp. at the Bermuda Atlantic Time-series Study (BATS) site, Deep Sea Research Part I, 48, 1583–1608, 2001.

Polerecky, L., Adam, B., Milucka, J., Musat, N., Vagner, T., and Kuypers, M. M. M.: Look@NanoSIMS – a tool for the analysis of nanoSIMS data in environmental microbiology., Environmantal Microbiology, 4, 1009-1023, 2012.

Pujo-Pay, M. and Raimbault, P.: Improvement of the wet-oxidation procedure for simultaneous determination of particulate organic nitrogen and phosphorus collected on filters, Marine and Ecological Progress Series, 105, 203-207, 1994.

Qi, H., Coplen, T. B., Geilmann, H., Brand, W. A., and Böhlke, J. K.: Two new organic reference materials for d13C and d15N measurements and a new value for the d13C of NBS 22 oil., Rapid Communications in Mass Spectrometry, 17, 2483–2487, 2003.

Rahav, E., Herut, B., Levi, A., Mulholland, M. R., and Berman-Frank, I.: Springtime contribution of dinitrogen fixation to primary production across the Mediterranean Sea, Ocean Sci, 9, 489-498, 2013.

Raveh, O., David, N., Rilov, G., and Rahav, E.: The temporal dynamics of coastal phytoplankton and bacterioplankton in the eastern Mediterranean Sea, , PloS one, In press, 2015.

Redfield, A. C.: On the proportions of organic derivations in sea water and their relation to the composition of plankton. In: James Johnstone Memorial Volume, R.J., D. (Ed.), University Press of Liverpool, 1934.

Rodier, M. and Le Borgne, R.: Population and trophic dynamics of Trichodesmium thiebautii in the SE lagoon of New Caledonia. Comparison with T. erythraeum in the SW lagoon, Marine Pollution Bulletin, 61, 349-359, 2010.

Rodier, M. and Le Borgne, R.: Population dynamics and environmental conditions affecting Trichodesmium spp. (filamentous cyanobacteria) blooms in the south-west lagoon of New Caledonia, Journal of Experimental Marine Biology and Ecology, 358, 20-32, 2008.

Scharek, R., Latasa, M., Karl, D. M., and Bidigare, R. R.: Temporal variations in diatom abundance and downward vertical fux in the oligotrophic North Pacific gyre, Deep Sea Research Part I, 46, 1051-1075, 1999a.

Sharek, R. M., Tupas, L. M., and Karl, D. M.: Diatom fluxes to the deep sea in the oligotrophic North Pacific gyre at Station ALOHA, Marine and Ecological Progress Series, 82, 55-67, 1999b.

Shiozaki, T., Nagata, T., Ijichi, M., and Furuya, K.: Nitrogen fixation and the diazotroph community in the temperate coastal region of the northwestern North Pacific, Biogeosciences, 12, 4751–4764, 2015.

Sigman, D. M., Casciotti, K. L., Andreani, M., Barford, C., Galanter, M., and Böhlke, J. K.: A bacterial method for the nitrogen isotopic analysis of nitrate in seawater and freshwater, Analytical Chemistry, 73, 4145–4153, 2001.

Smayda, T. J.: What to count. In Phytoplankton Manual, ed. . In: Monographs on oceanographic methodology 6, Sournia, A. (Ed.), UNESCO, Paris, 1978.

Sohm, J. A. and Capone, D. G.: Phosphorus dynamics of the tropical and subtropical north Atlantic: *Trichodesmium* spp. versus bulk plankton, Marine and Ecological Progress Series, 317, 21-28, 2006.

Staal, M., Meysman, F. J., and Stal, L. J.: Temperature excludes N2-fixing heterocystous cyanobacteria in the tropical oceans., Nature, 425, 504-507, 2003.

Subramaniam, A., Yager, P. L., Carpenter, E. J., and al., e.: Amazon River enhances diazotrophy and carbon sequestration in the tropical North Atlantic Ocean., Proceedings of the National Academy of Sciences, 105, 10460–10465, 2008.

Sun, J. and Liu, D.: Geometric models for calculating cell biovolume and surface area for phytoplankton, Journal of Plankton Research, 25, 1331-1346, 2003.

Thompson, A., Carter, B. J., Turk-Kubo, K., Malfatti, F., Azam, F., and Zehr, J. P.: Genetic diversity of the unicellular nitrogen-fixing cyanobacteria UCYN-A and its prymnesiophyte host, Environmental microbiology, 16, 3238–3249, 2014.

Tripp, H. J., Bench, S. R., Turk, K. A., Foster, R. A., Desany, B. A., Niazi, F., Affourtit, J. P., and Zehr, J. P.: Metabolic streamlining in an open-ocean nitrogen-fixing cyanobacterium, Nature, 464, 90-94, 2010.

Turk-Kubo, K. A., Frank, I. E., Hogan, M. E., Desnues, A., Bonnet, S., and Zehr, J. P.: Diazotroph community succession during the VAHINE mesocosms experiment (New Caledonia Lagoon), Biogeosciences, 12, 7435-7452, 2015.

Van Wambeke, F., Pfreundt, U., Barani, A., Berthelot, H., Moutin, T., Rodier, M., Hess, W., and Bonnet, S.: Heterotrophic bacterial production and metabolic balance during the VAHINE mesocosm experiment in the New Caledonia lagoon Biogeosciences Discussions, 12, 19861-19900, 2015.

Verity, P. G., Robertson, C. Y., Tronzo, C. R., Andrews, M. G., Nelson, J. R., and Sieracki, M. E.: Relationships between cell volume and the carbon and nitrogen content of marine photosynthetic nanoplankton, Limnology and Oceanography, 37, 1434–1446, 1992.

Vincent, D., Slawyk, G., L'Helguen, S., Sarthou, G., Gallinari, M., Seuront, L., Sautour, B., and Ragueneau, O.: Net and gross incorporation of nitrogen by marine copepods fed on 15N-labelled diatoms: Methodology and trophic studies, Journal of experimental marine biology and ecology, 352, 295-305, 2007.

Walsby, A. E.: The gas vesicles and buoyancy of *Trichodesmium*, Marine Pelagic Cyanobacteria: Trichodesmium and other Diazotrophs, 1992. 141-161, 1992.

White, A. E., Foster, R. A., Benitez-Nelson, C. R., Masqué, P., Verdeny, E., Popp, B. N., Arthur, K. E., and Prahl, F. G.: Nitrogen fixation in the Gulf of California and the Eastern Tropical North Pacific, Progess in Oceanography, 109, 1-17, 2012.

Wilson, S. T., Böttjer, D., Church, M. J., and Karl, D. M.: Comparative assessment of nitrogen fixation methodologies conducted in the oligotrophic Noth Pacific Ocean, Applied and Environmental Microbiology, 78, 6516–6523, 2012.

Yentsch, C. S. and Phinney, D. A.: Spectral fluorescence: An ataxonomic tool for studying the structure of phytoplankton populations, Journal of Plankton Research, 7, 617–632, 1985.

Zehr, J. P., Bench, S. R., Carter, B. J., Hewson, I., Niazi, F., Shi, T., Tripp, H. J., and Affourtit, J. P.: Globally Distributed Uncultivated Oceanic N_2-Fixing Cyanobacteria Lack Oxygenic Photosystem II, Science, 322, 1110-1112, 2008.

Table 1. N_2 fixation rates (nmol N L^{-1} d^{-1}) measured in the mesocosms and in lagoon waters. Table shows the range, median, mean, contribution of the <10 µm fraction to total rates (%), and the number of samples analysed (n).

	Range	Median	Mean	% <10 µm	n
M1	0.5-69.7	15.9	19.7	38	61
M2	3.0-67.7	15.1	18.1	43	57
M3	2.9-60.4	14.2	17.7	29	59
Average mesocosms	2.1-65.9	15	18.5	37	177
Lagoon waters	1.9-29.3	8.7	9.2	n.a	61

Table 2. Spearman correlation matrix of N_2 fixation rates and hydrological parameters, biogeochemical stocks and fluxes, and planktonic communities (n=66). The significant correlations ($p<0.05$) are indicated in bold. n.a- not available.

	Parameter	M1	M2	M3	Lagoon waters
Hydrological parameters	Temperature	**0.394**	**0.319**	**0.347**	0.228
	Salinity	0.211	0.213	**0.266**	-0.122
Biogeochemical stocks and fluxes	NO_3^-	**-0.539**	**-0.302**	**-0.341**	0.145
	NH_4^+	0.152	0.103	0.006	0.197
	DIP	**-0.613**	**-0.569**	**-0.482**	-0.116
	DON	**-0.329**	**-0.413**	-0.235	-0.180
	DOP	**-0.563**	-0.157	**-0.316**	-0.243
	PON	**0.575**	**0.293**	**0.494**	0.077
	POP	**0.514**	0.001	**0.439**	0.036
	POC	**0.399**	**0.352**	**0.356**	-0.061
	Chl *a*	**0.660**	**0.656**	**0.656**	0.220
	Primary production	**0.443**	**0.498**	**0.445**	**0.268**
	Bacterial production	**0.708**	**0.408**	**0.471**	0.189
	T-DIP	**-0.670**	**-0.603**	**-0.564**	-0.190
	APA	**0.575**	**0.568**	**0.273**	-0.062
Planktonic communities	HNA	**0.317**	-0.043	**0.458**	n.a
	LNA	0.262	-0.021	0.000	n.a
	Prochlorococcus	**0.429**	-0.122	0.138	n.a
	Synechococcus	**0.699**	**0.434**	**0.499**	n.a
	Pico-eukaryotes	**0.614**	**0.563**	**0.414**	n.a
	Nanoeukaryotes	**0.477**	0.002	**0.442**	n.a
	Diatoms	-0.099	0.456	-0.200	n.a
	Dinoflagellates	0.242	-0.392	-0.321	n.a
	UCYN-A1	0.545	-0.521	-0.503	0.200
	UCYN-A2	0.127	**-0.631**	0.248	0.333
	UCYN-B	0.083	**0.696**	0.467	0.101
	UCYN-C	0.373	**0.621**	0.515	-0.167
	Trichodesmium	-0.145	0.147	0.285	-0.117
	DDAs	-0.036	-0.264	-0.527	0.262
	γ-24774A11	0.327	0.497	**-0.750**	**0.733**

Table 3. Average NO_3^-, DIP, DON, and DOP concentrations (µmol L^{-1}) measured over the P0, P1 and P2 periods. NO_3^- and DIP concentrations were determined using a segmented flow analyzer according to (Aminot and Kerouel, 2007). The detection limit was 0.01 and 0.005 µmol L^{-1} for NO_3^- and DIP, respectively. DON and DOP concentrations were determined according to the wet oxidation procedure described in Pujo-Pay and Raimbault (1994) and Berthelot et al. (2015b).

	Average P0	Average P1	Average P2
NO_3^-	0.04±0.02	0.03±0.01	0.02±0.01
DIP	0.03±0.01	0.48±0.20	0.08±0.05
DON	5.19±0.37	5.22±0.54	4.73±0.49
DOP	0.14±0.01	0.16±0.03	0.12±0.02

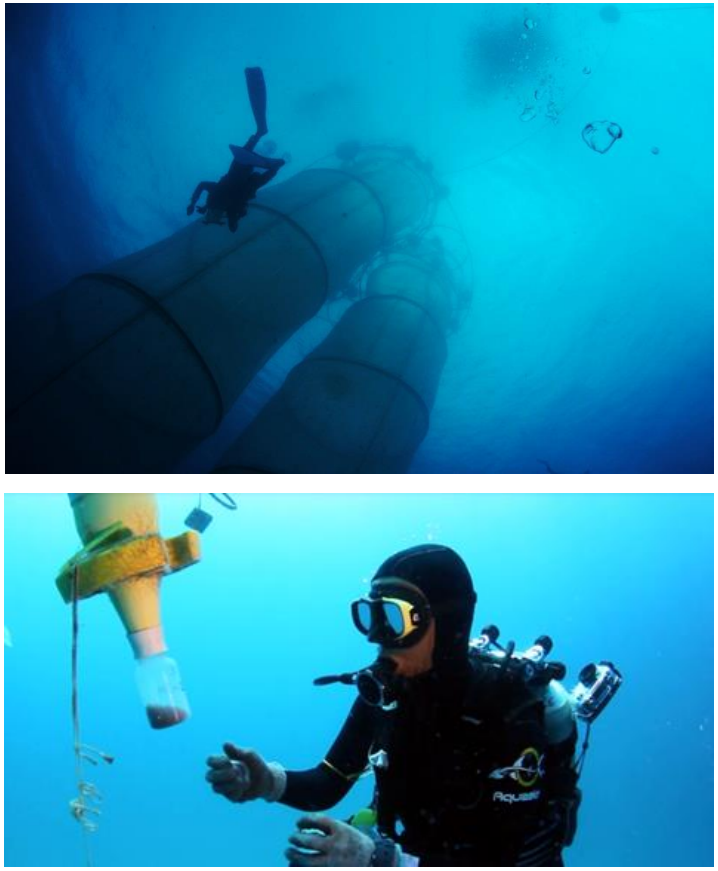

Figure 1.

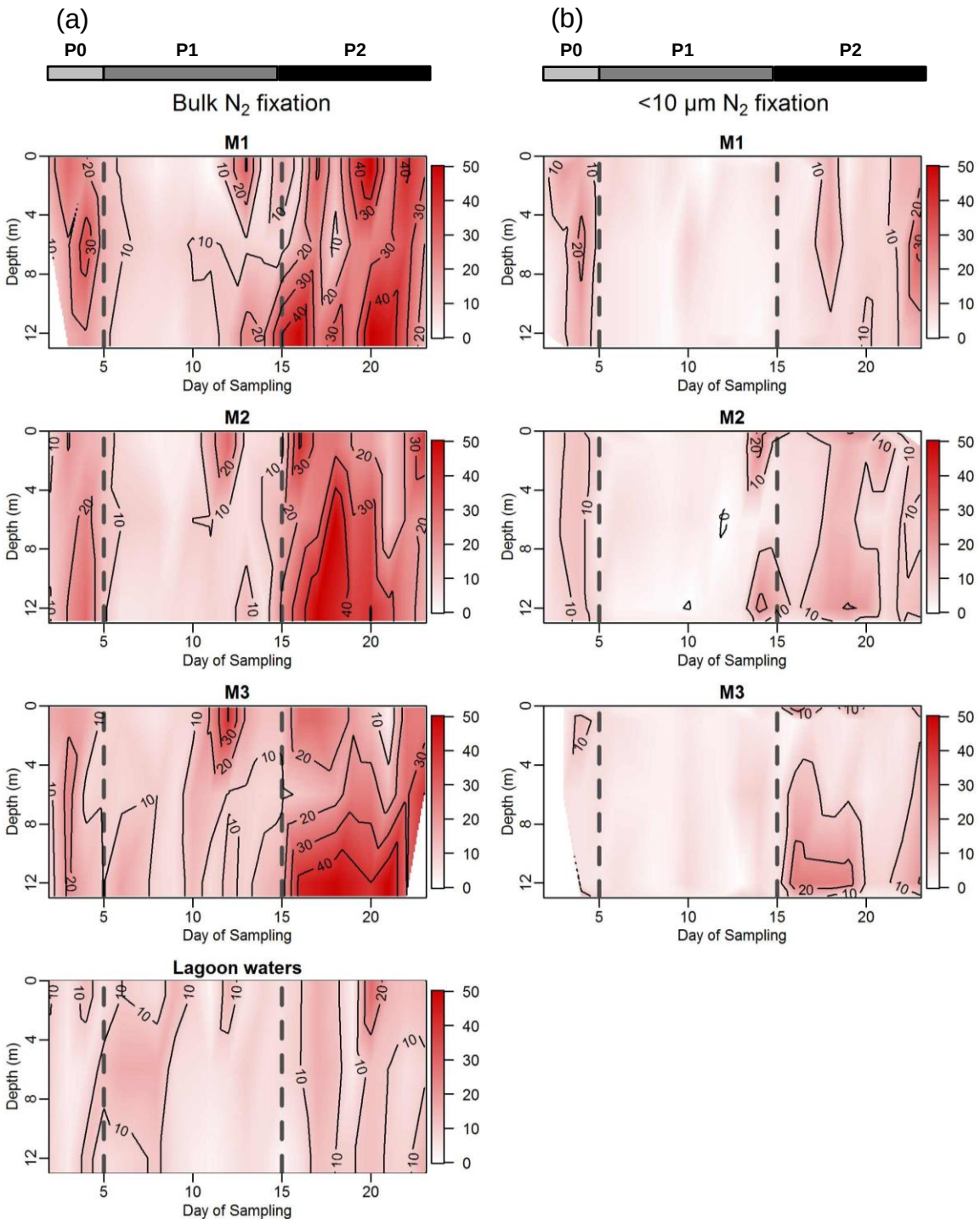
(a)
P0
P1
P2
Bulk N_2 fixation
M1
M2
M3
Lagoon waters
(b)
P0
P1
P2
<10 µm N_2 fixation
M1
M2
M3
Depth (m)
Day of Sampling

Figure 2.

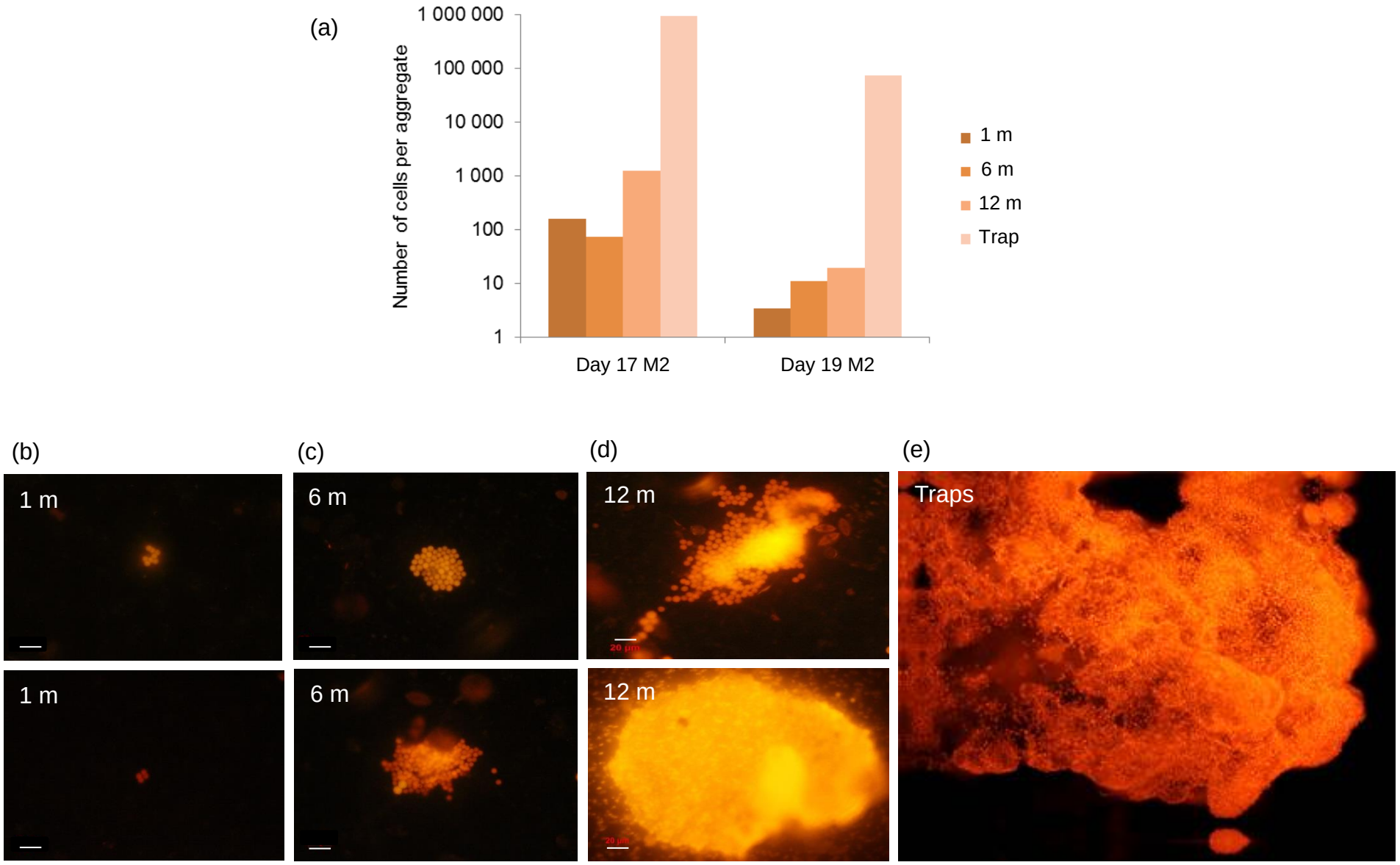
(a)
1 000 000
100 000
10 000
1 000
100
10
1
Number of cells per aggregate
Day 17 M2
Day 19 M2
1 m
6 m
12 m
Trap
(b)
(c)
(d)
(e)
1 m
1 m
6 m
6 m
12 m
12 m
Traps

Figure 3.

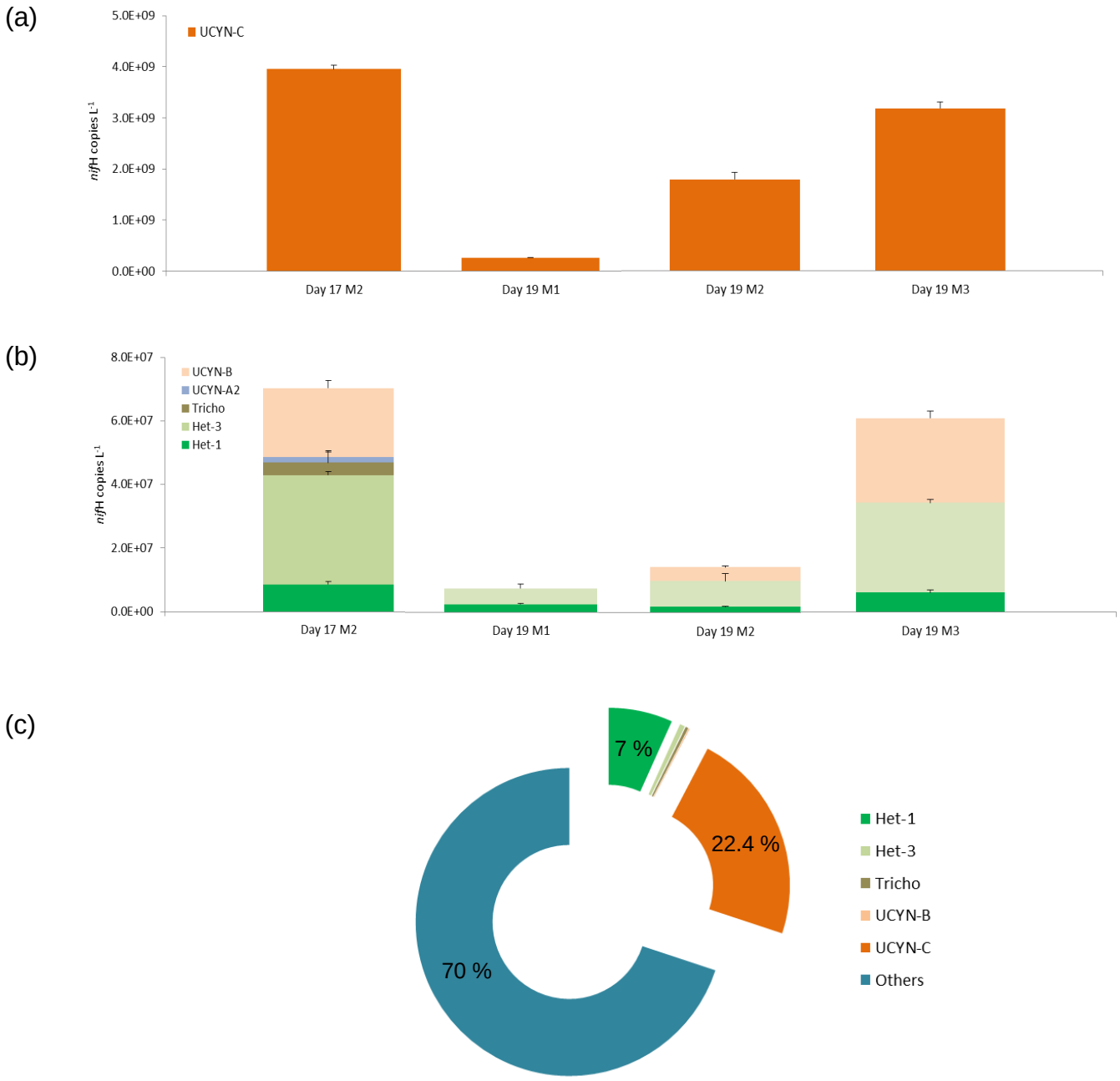
(a)
UCYN-C
5.0E+09
4.0E+09
3.0E+09
2.0E+09
1.0E+09
0.0E+00
nifH copies L-1
Day 17 M2
Day 19 M1
Day 19 M2
Day 19 M3
(b)
UCYN-B
UCYN-A2
Tricho
Het-3
Het-1
8.0E+07
6.0E+07
4.0E+07
2.0E+07
0.0E+00
nifH copies L-1
Day 17 M2
Day 19 M1
Day 19 M2
Day 19 M3
(c)
7 %
22.4 %
70 %
Het-1
Het-3
Tricho
UCYN-B
UCYN-C
Others

Figure 4.

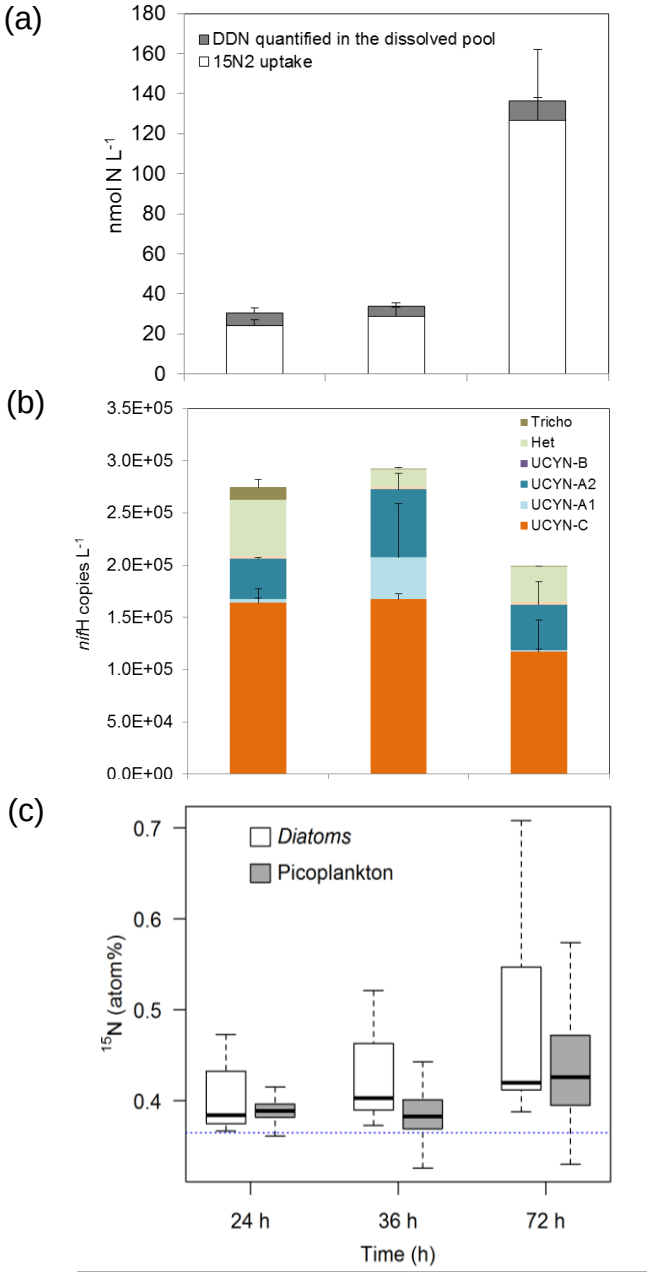
(a)
DDN quantified in the dissolved pool
15N2 uptake
nmol N L-1
180
160
140
120
100
80
60
40
20
0
(b)
Tricho
Het
UCYN-B
UCYN-A2
UCYN-A1
UCYN-C
nifH copies L-1
3.5E+05
3.0E+05
2.5E+05
2.0E+05
1.5E+05
1.0E+05
5.0E+04
0.0E+00
(c)
Diatoms
Picoplankton
15N (atom%)
0.7
0.6
0.5
0.4
24 h
36 h
72 h
Time (h)

Figure 5.

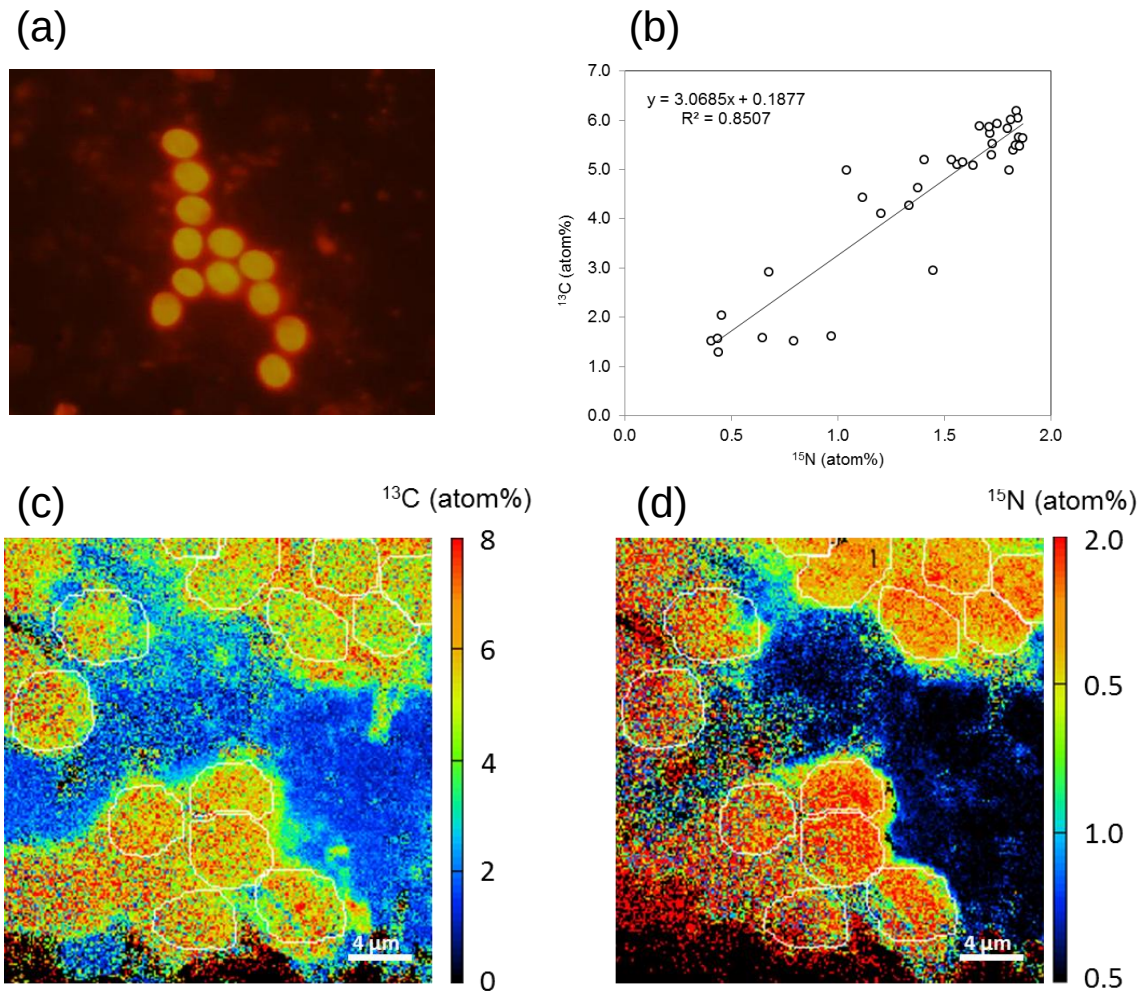
(a)
(b)
y = 3.0685x + 0.1877
R² = 0.8507
13C (atom%)
15N (atom%)
7.0
6.0
5.0
4.0
3.0
2.0
1.0
0.0
0.0
0.5
1.0
1.5
2.0
(c)
13C (atom%)
8
6
4
2
0
4 µm
(d)
15N (atom%)
2.0
0.5
1.0
0.5
4 µm

Figure 6.

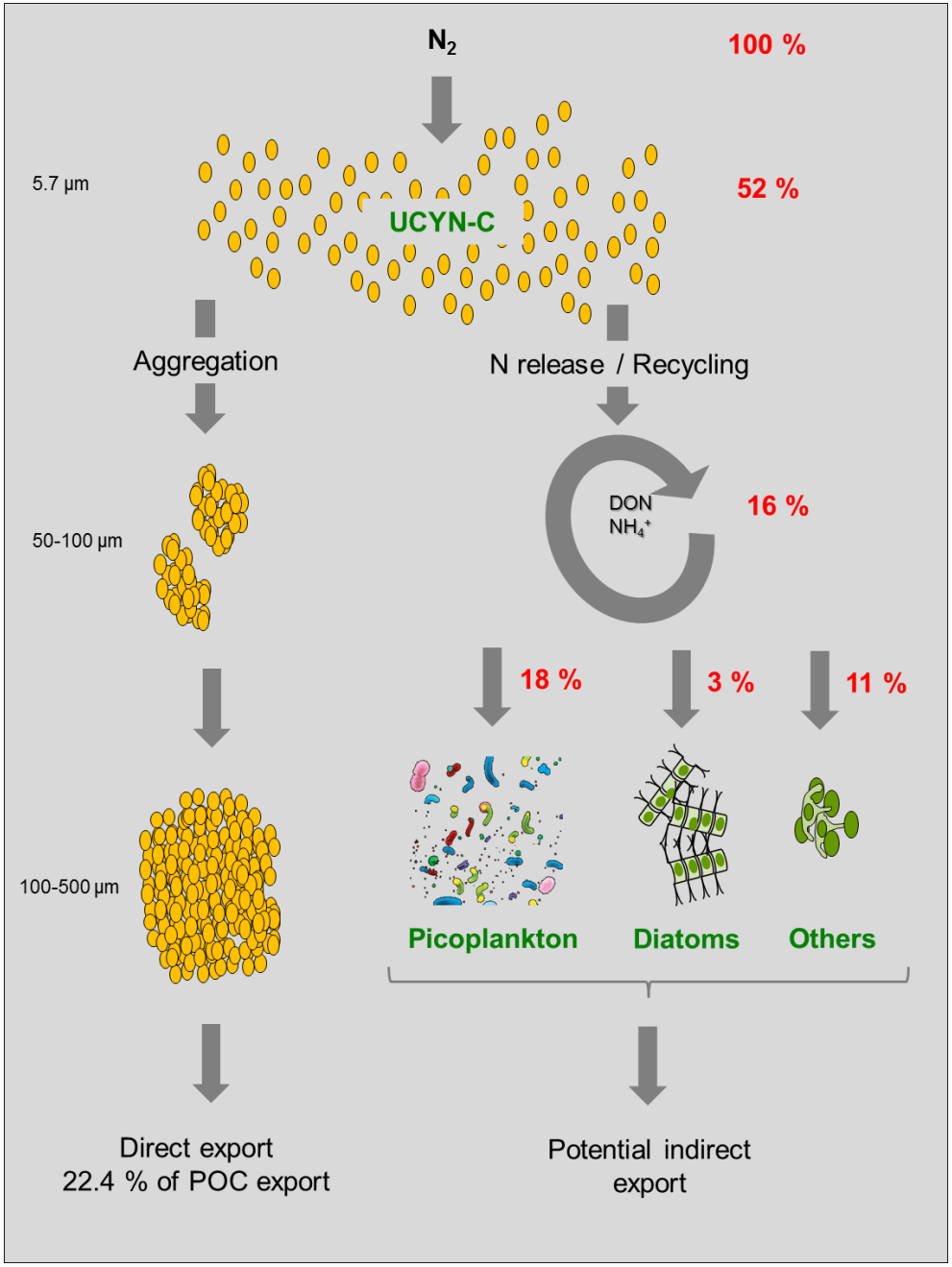
N_2
100 %
5.7 µm
UCYN-C
52 %
Aggregation
N release / Recycling
50-100 µm
DON
NH_4^+
16 %
18 %
3 %
11 %
100-500 µm
Picoplankton
Diatoms
Others
Direct export
22.4 % of POC export
Potential indirect
export

Figure 7.